Cavefish cope with environmental hypoxia by developing more erythrocytes and overexpression of hypoxia inducible genes

Running Title: Cavefish response to hypoxia

Corine M. van der Weele and William R. Jeffery

Department of Biology, University of Maryland, College Park, MD 20742 USA

Correspondence: Jeffery@umd.edu

Keywords

Hypoxia, *Astyanax mexicanus*, Cavefish, Hematopoiesis, Erythrocytes, Hypoxia-inducible genes, Cave colonization.

Summary

Astyanax mexicanus cavefish cope with hypoxic environments by expanding embryonic hematopoietic domains, increasing the capacity for erythrocyte development, and constitutive overexpression of hypoxia-inducible genes.

Abstract

Dark caves lacking primary productivity can expose subterranean animals to hypoxia. We used the surface-dwelling (surface fish) and cave-dwelling (cavefish) morphs of *Astyanax mexicanus* as a model for understanding the mechanisms of hypoxia tolerance in the cave environment. Primitive hematopoiesis, which is restricted to the posterior lateral mesoderm in other teleosts, also occurs in the anterior lateral mesoderm in *Astyanax*, potentially pre-adapting surface fish for hypoxic cave colonization. Cavefish have enlarged both hematopoietic domains and develop more erythrocytes than surface fish, which are required for normal development in both morphs. Laboratory induced hypoxia suppresses growth in surface fish but not in cavefish. Both morphs respond to hypoxia by overexpressing Hypoxia-Inducible Factor (HIF) pathway genes, but some *hif* genes are constitutively upregulated in normoxic cavefish to similar levels as hypoxic surface fish. We conclude that cavefish cope with hypoxia by increasing erythrocyte development and constitutive HIF gene overexpression.

Introduction

A unifying theme of cave habitats is complete darkness (Culver and Pipan, 2009) and the absence of primary productivity can subject cave-dwelling animals to oxygen deficiency (Malard and Hervant, 1999). We have used the teleost *Astyanax mexicanus*, which consists of surface-dwelling (surface fish) and cave-dwelling (cavefish) morphs, as a model to study adaptation to hypoxia in caves. Surface fish colonized subterranean waters in the Sierra de El Abra region of Mexico (Mitchell et al., 1977; Gross, 2012) during the late Pleistocene (Fumey et al., 2018;

47 Herman et al., 2018), and their cavefish descendants evolved numerous traits for adaptation to
48 perpetual darkness. Cavefish adaptations include more taste buds and cranial neuromasts,
49 increased olfactory capacity, and fat deposits, which could facilitate feeding and survival during
50 times of low food input, and decreased metabolic rates and loss of eyes, which may be important
51 in energy conservation (Yamamoto et al., 2004; Moran et al., 2014; 2015, Varatharasan et al.,
52 2009; Blin et al., 2018; Yoshizawa et al., 2014; Hüppop, 1986; Xiong et al., 2018). Hypoxia
53 may be a deterrent to the survival of colonizing teleosts in the Sierra de El Abra, where oxygen
54 reductions of 50% or more have been measured in cave waters (Boggs and Gross, 2021; Rohner
55 et al., 2013, Ornelas-Garcia et al., 2018). *Astyanax* cavefish thrive under these conditions, but
56 little is known about how they have adapted to hypo-oxygenated waters.

57 Oxygen is bound to hemoglobin and transported through the body by red blood cells.
58 Increased erythrocyte production is a well-documented strategy for coping with hypoxia at high
59 altitude (Haase, 2013), but the role of red blood cells in adaptation to hypoxic caves is unknown.
60 Hematopoiesis, the process in which erythrocytes and other blood cells develop during
61 embryogenesis, occurs in two waves in vertebrates: the primitive and definitive waves (Davidson
62 and Zon, 2004; Paik and Zon, 2010). In the zebrafish *Danio rerio* and other teleost embryos, the
63 first or primitive wave occurs in the anterior and posterior lateral mesoderm beginning during the
64 tailbud stage. The anterior lateral mesoderm (ALM) undergoes myelopoiesis to form
65 macrophages, and some of these later differentiate into neutrophils and microglia (Herbomel et
66 al., 1999; Herbomel et al., 2001; Le Guyader et al., 2008), whereas the posterior lateral
67 mesoderm (PLM) undergoes erythropoiesis to form primitive erythrocytes. Subsequently, the
68 PLM converges into the intermediate cell mass, where the precursors of endothelial cells lining
69 the first blood vessels, primitive erythrocytes, and myeloid cells will ultimately differentiate.

70 The second or definitive wave of hematopoiesis begins later in development when hematopoietic
71 stem and progenitor cells are formed in the aorta-gonad-mesonephros (AGM), which seed the
72 caudal hematopoietic tissue and form the posterior blood islands, where definitive erythrocytes
73 begin to differentiate (Paik and Zon 2010; Gore et al., 2018). Eventually, definitive
74 hematopoiesis moves to the thymus and head kidneys in adults. The primitive and definitive
75 waves of hematopoiesis are potential targets for adaptive changes induced by hypoxia.
76 Hematopoiesis is directed by a series of transcription factors producing different types of
77 blood cells (Davidson and Zon, 2004; Carroll and North, 2014). The *growth factor*
78 *independence 1* (*gfi1aa*) gene, which encodes a transcriptional repressor of many different genes
79 (Möröy et al., 2015), is important for primitive hematopoiesis at several developmental stages
80 (Wei et al., 2008; Cooney et al., 2013; Moore et al., 2018). In zebrafish, *gfi1aa* expression occurs
81 throughout the period of embryonic segmentation, first in the PLM, then in the intermediate cell
82 mass, and finally in the AGM (Wei et al., 2008; Cooney et al., 2013), where it directs the
83 development of hemogenic endothelia into hematopoietic stem and progenitor cells, which
84 ultimately differentiate into red blood cells (Moore et al., 2018). The *gfi1aa* gene is also
85 expressed in the ALM, albeit weakly and only for a short time (Wei et al., 2008). Its expression
86 at different stages of hematopoiesis makes *gfi1aa* an excellent marker for investigating
87 differences between surface fish and cavefish hematopoiesis. The *LIM domain only 2* gene
88 encodes another transcription factor essential for determination of hematopoietic domains early
89 in primitive hematopoiesis (Patterson et al., 2007) and is also an excellent marker for differences
90 during the initial stages of hematopoiesis.
91 Oxygen is required in aerobic organisms to produce energy, and insufficient oxygen leads
92 to the activation of an evolutionarily-conserved transcriptional response (Majmundar et al.,

2010). The responses to oxygen deprivation are coordinated by activation of the hypoxia-inducible factors (HIF1, HIF2 and HIF3) (Semenza and Wang, 1992), a family of transcription factors controlling a large number of downstream target genes involved in promoting different responses to hypoxia (Pelster and Egg, 2018; Rashid et al., 2017). Increased expression of the α subunit of HIF1 and the HIF regulated genes are indicators of hypoxia (Mandic et al., 2021). Notable responses include the improvement of oxygen supply through increasing red blood cell production and function (Haase, 2013; Kulkarni et al., 2010; Cai et al., 2020), metabolic homeostasis balancing ATP production with oxygen consumption, management of Reactive Oxygen Species (ROS) via glycolysis, modulating anaerobic respiration and the pentose phosphate pathway (PPP) (Singh et al., 2017; Wheaton and Chandel, 2011; Stincone et al., 2015), and conservation of energy by growth inhibition (Kamei, 2020). *Astyanax* cavefish (Hüppop, 1986; Moran et al., 2014, Aspiras et al., 2015) and other cave-adapted animals (Bishop et al., 2004) have evolved reduced metabolic rates to conserve energy in the cave environment. However, the strategies used to conserve energy in hypoxic cave environments are poorly understood.

The present investigation shows that cavefish embryos develop significantly more erythrocytes than surface fish. The results also revealed that cavefish larvae have constitutively high expression of some of the HIF1 pathway genes and show no effects of oxygen depletion on growth, traits that could promote larval survival in hypoxic environments. These studies reveal that changes in development of the circulatory system may underlie adaptation of cavefish to hypo-oxygenated environments.

Results

116

117 *Cavefish have more erythrocytes than surface fish*

118 To test the hypothesis that cavefish develop more red blood cells as a response to
119 environmental hypoxia, we compared erythrocytes between surface fish and cavefish embryos in
120 several different ways. First, we conducted direct observations of blood cell numbers after
121 circulation begins in the Duct of Cuvier (DC) at 36 hpf (Fig. 1A-D). At this time, the circulatory
122 system is still partially open, and blood cells can be imaged or stained and quantified as they
123 flow across the yolk (Videos 1, 2 and Fig. 1B-D, F). The number of circulating blood cells was
124 quantified in sequential video frames using Image-J analysis software, and the results showed
125 that cavefish have more blood cells than surface fish (Fig. 1B-D, F). Second, the number of
126 erythrocytes was quantified in the DC by staining with o-dianisidine (Iuchi and Yamamoto,
127 1983), and the results revealed that cavefish have more erythrocytes than surface fish (Fig. 1E,
128 G). Third, expression of the *hbb2* and *hbbe2 ß-hemoglobin* genes was followed during surface
129 fish and cavefish development by qPCR and *in situ* hybridization (Fig. 2A, B, D-F). The qPCR
130 results revealed significantly higher levels of *hbb2* mRNA at 24 hpf and 60 hpf and *hbbe2*
131 mRNA at 60 hpf (Fig. 2 A, B). *In situ* hybridization also showed more extensive *hbb2* staining
132 in cavefish compared to surface fish (Fig. 2D-F), which was particularly evident in the yolk mass
133 at 36 hpf (Fig. 2E). Fourth, the expression of *gfi1aa*, which encodes a transcription factor
134 essential for hematopoiesis (Cooney et al., 2013), was compared by qPCR and *in situ*
135 hybridization (Fig. 2C, G). The results indicated that *gfi1aa* mRNA levels were significantly
136 increased in cavefish compared to surface fish at 24 hpf (Fig. 2C, G), prior to detection of the
137 highest levels of hemoglobin transcription (Fig. 2A, B). These results provide multiple lines of
138 evidence indicating that red blood cells are increased during cavefish development.

139

140 *Hematopoietic domains in surface fish and cavefish embryos*

141 To determine the developmental basis of erythrocyte enhancement, we compared the
142 timing and spatial expression of *hbb2*, *gfi1aa,* and other hematopoietic marker genes during
143 primitive hematopoiesis in surface fish and cavefish embryos (Fig. 3). As in zebrafish (Brownlie
144 et al., 2003; Wei et al., 2008), *hbb2* was expressed in the intermediate cell mass of the PLM
145 during primitive hematopoiesis in *Astyanax* surface fish and cavefish embryos (Fig. 3A). In
146 striking contrast to zebrafish, in which erythropoiesis occurs exclusively in the PLM, *hbb2*
147 expression was detected in both the ALM and PLM of *Astyanax* surface fish and cavefish
148 embryos (Fig. 3A). The expression of *gfi1aa* was also present in the ALM and PLM during
149 *Astyanax* embryogenesis (Fig. 3A). Furthermore, *gfi1aa* and *hbb2* staining were stronger in the
150 cavefish ALM and PLM compared to surface fish (Fig. 3A). To further evaluate the primitive
151 erythropoietic domains, we examined expression of the *lim domain only 2* (*lmo2*) gene, a marker
152 of developing blood cells (Patterson et al., 2007), by *in situ* hybridization. The results confirmed
153 blood cell development in both the ALM and PLM in *Astyanax* embryos and revealed that both
154 primitive erythropoietic domains are expanded in cavefish embryos (Fig. 3C).

155 In zebrafish, the ALM undergoes myelopoiesis, rather than erythropoiesis, producing
156 macrophages that disperse throughout the embryo (Herbomel et al., 1999). Therefore, we asked
157 if macrophage development in *Astyanax* is compromised by the expansion of primitive
158 erythropoiesis into the ALM. To address this possibility, we examined expression of the *l-*
159 *plastin1* (*lcp1*) gene, a marker for macrophage differentiation (Herbomel et al., 2001). *In situ*
160 hybridization showed that *lcp1* expressing cells were distributed throughout the ventral body and
161 yolk masses of surface fish and cavefish embryos, implying that macrophages migrated from the

162 ALM and differentiated (Fig. 2B). Therefore, macrophage development does not appear to be
163 compromised by the expansion of erythropoiesis into the ALM.
164 In summary, the results reveal the presence of a novel domain of primitive erythropoiesis
165 in the anterior region of *Astyanax* embryos and suggest that red blood cells are increased in
166 cavefish due to expansion of both the anterior and posterior primitive erythropoiesis domains.
167
168 *Blood cell enhancement is a maternally controlled trait*
169 Hematopoietic domains develop in the lateral mesoderm of zebrafish embryos during
170 gastrulation (Kimmel et al., 1990), and changes in gastrulation and axis determination are under
171 maternal control in cavefish (Ma et al., 2018; Torres-Paz et al., 2019). Therefore, to determine
172 whether the increase in cavefish blood cells is controlled by maternal or zygotic changes, we
173 conducted reciprocal hybrid crosses (cavefish female x surface male and surface fish female x
174 cavefish male) and quantified blood cells in the DC of F1 hybrid embryos by video imaging (Fig.
175 4). As controls, crosses were also done and blood cell numbers quantified in the offspring of
176 parental cavefish x cavefish and surface fish x surface fish crosses. The F1 hybrid progeny of
177 the cavefish female x surface fish male and the cavefish x cavefish crosses (Fig. 4C, D)
178 developed more blood cells than the progeny of surface fish female x cavefish male and surface
179 fish x surface fish crosses (Fig. 4A, B), showing that the extent of erythrocyte development is
180 dependent on the source of eggs. These results reveal that the increase in cavefish blood cells is
181 a maternally controlled trait.
182
183 *Erythrocytes are required for Astyanax development*

184 Erythrocytes also develop early in zebrafish embryogenesis, but are not required for
185 oxygen delivery until much later in development (Pelster and Burggren, 1996). Accordingly, we
186 performed experiments to determine whether red blood cells have a role in early *Astyanax*
187 development. To address this question, we compared the effects of hemolytic anemia in surface
188 fish and cavefish embryos (Fig. 5). Hemolysis of red blood cells was induced by treatment with
189 phenylhydrazine (PHZ) (Houston et al., 1988) beginning at 14 hpf (13-17 somite stage), and
190 *hbb2* staining, red blood cell number, and post-anal tail length (used as a proxy for normal
191 growth and development) were compared in surface fish and cavefish 14 hrs. later (Fig. 5A-C).
192 We found that *hbb2* staining and red blood cells were reduced at increasing PHZ concentrations
193 in both surface fish and cavefish embryos (Fig. 5A, B). However, at the same PHZ concentration
194 both erythrocyte phenotypes were more strongly affected in surface fish than in cavefish,
195 consistent with more red blood cells in the latter. The results also showed that growth decreased
196 in concert with hemoglobin transcript and erythrocyte reduction in surface fish, and concordant
197 with more red blood cells, no effects on growth were seen in PHZ-treated cavefish (Fig. 5B).
198 The PHZ-treated embryos developed axial defects, most notably edemas, twisted notochords,
199 and shortened and ventrally bent tails (Fig. 5C), which were more prevalent at lower PHZ
200 concentrations in surface fish than cavefish embryos (Table 1). To address the possibility that
201 reduced tail length was a consequence of abnormal notochord morphogenesis rather than growth
202 suppression, tail length and notochord morphology were investigated at 36 hpf in surface fish
203 exposed to a PHZ concentration that virtually abolished red blood cells (Fig. 5D). Under these
204 conditions, post-anal tail growth was significantly reduced, but notochord defects were not
205 detected, suggesting that hemolytic effects on axial growth are related to the absence of red

206 blood cells. The results show that erythrocytes are required during early development in
207 *Astyanax* and more red blood cells may reduce the sensitivity of cavefish to hemolytic anemia.
208
209 *Cavefish but not surface fish maintain growth in a hypoxic laboratory environment*
210 Subterranean waters harboring *Astyanax* cavefish are low in oxygen (Rohner et al., 2013;
211 Ornelas-Garcia et al., 2018; Boggs and Gross, 2021), which is essential for normal development
212 and growth (Giaccia et al., 2004). Therefore, we hypothesized that cavefish may be more
213 tolerant to the effects of hypoxia on growth than surface fish. To test this hypothesis, 36 hpf
214 surface fish and cavefish were exposed to a hypoxic laboratory environment for 18 hours (Fig.
215 6A, B). The effects on growth were determined by measuring post-anal tail length before and
216 after hypoxia treatment, and the number of erythrocytes was quantified by o-dianisidine staining
217 at the end of the treatment period. The results showed that hypoxia reduced the number of red
218 blood cells in the DC and suppressed growth in surface fish but not cavefish (Fig. 6B), showing
219 that cavefish are more resistant to oxygen depletion. Reasoning that eye growth would be
220 especially sensitive to hypoxia because of the energy cost associated with retinal differentiation
221 and maintenance (Wong-Riley, 2010; Moran et al., 2015), eye size was also examined in surface
222 fish and cavefish exposed to normoxia or hypoxia for 18 hrs. The results showed that eye size
223 was more sensitive to hypoxia relative to normoxia in surface fish compared to cavefish (Fig.
224 6C). The results suggest that cavefish growth is resistant to hypoxia and development of more
225 erythrocytes may contribute to hypoxia tolerance.
226
227 *Differential expression of oxygen-sensitive genes during hypoxia*

228 To determine the molecular responses of surface fish and cavefish to hypoxia, we
229 quantified some of the key oxygen sensitive genes by qPCR (Fig. 7). Exposure of surface fish or
230 cavefish larvae to hypoxia for 2 hrs. resulted in increased transcript levels of the *insulin growth*
231 *factor binding protein 1a* (*igfbp1a*) gene, the HIF1 family genes *hif1aa* and *hif1a-like2*, and the
232 HIF1-regulated downstream gene *hexokinase 1* (*hk1*) (Fig. 7). In contrast, the *hifab* and *hif1a-*
233 *like* genes were expressed at similar levels in normoxic cavefish and hypoxic surface fish (Fig.
234 7), implying constitutive expression in cavefish. The expression of the *glucose-6-phosphate*
235 *dehydrogenase* (*g6pd*), *lactate dehydrogenase a* (*ldha*), and *pyruvate dehydrogenase kinase 1*
236 (*pdk1*) genes were not significantly increased by hypoxia in surface fish or cavefish (Fig. 7). The
237 results indicate that *igfbp1*, *hif1a-like2* and *hk1* are upregulated by hypoxia in both surface fish
238 and cavefish, whereas *hif1aa* and *hif1a-like* are expressed at higher levels in cavefish than in
239 surface fish in either normoxic or hypoxic laboratory conditions. Thus, cavefish exhibit a
240 complex molecular response to hypoxia: some oxygen sensing genes are upregulated, others are
241 not changed, and some of the latter genes may be insensitive to oxygen depletion because they
242 are already expressed at maximal levels in normoxic cavefish.
243
244 **Discussion**
245
246 We show that cavefish embryos develop more red blood cells than surface fish embryos,
247 a classic response to hypoxia (Martinez, 2004; Timmerman and Chapman, 2004; Rutjes et al.,
248 2007; Haase, 2013), when they are raised under normoxic laboratory conditions. This conclusion
249 is based on direct counts of blood cells, including erythrocytes, increased expression of multiple
250 erythropoietic marker genes, and hyper-expression of the *gfi1aa* gene, a crucial regulator of

251 hematopoiesis. In addition, we report that the increase in erythrocytes may be caused by
252 expansion of embryonic hematopoietic domains in cavefish compared to surface fish. Finally,
253 we provide evidence that cavefish have evolved a permanent response to hypoxia involving the
254 constitutive overexpression of the some of the *hif1* genes, which persists under normoxic
255 laboratory conditions.

256 Hematopoiesis occurs in the primitive and definitive waves in vertebrates (Davidson and
257 Zon, 2004; Paik and Zon, 2010). Increased *hbb2, hbbe2,* and *gfi1aa* expression was observed
258 during embryogenesis and after larval hatching in cavefish. In zebrafish, transfusion experiments
259 indicate that blood cells circulating during the first four days of development are primitive
260 erythrocytes (Weinstein et al., 1996). Accordingly, our findings suggest that *Astyanax* larval
261 blood cells are primitive erythrocytes derived from the first wave of hematopoiesis.
262 Nevertheless, we also found stronger expression of erythropoietic marker genes in the AGM and
263 caudal hematopoietic tissue, which are involved in definitive hematopoiesis, implying that the
264 second wave may also be expanded in cavefish. Further investigation will be required to
265 determine whether erythrocytes are also increased in adults, although this possibility seems
266 likely because adult cavefish have increased levels of hemoglobin transcripts (Sears et al., 2020)
267 and more erythrocytes in their head kidneys compared to surface fish (Peuß et al., 2020). We
268 conclude that cavefish have evolved a permanent enhancement in red blood cells as a potential
269 adaptation for survival in hypoxic cave waters.

270 The results showed that surface fish and cavefish primitive erythrocytes are derived from
271 two different hematopoietic domains, one located anteriorly in the ALM and the other posteriorly
272 in the PLM. Importantly, both the anterior and posterior embryonic domains show expanded
273 marker gene expression in cavefish compared to surface fish. It is noteworthy that expansion of

274 the posterior hematopoietic domain can also be induced in zebrafish by overexpressing LMO2
275 together with its partner transcription factor SCL/TAL1 (Gering et al., 2003), suggesting that
276 teleosts have the capacity to modulate blood cell numbers by changing the size of primitive
277 erythropoietic domains during development. The existence of erythrocyte forming capacity in the
278 ALM of surface fish, albeit smaller than in cavefish, suggests that the expansion of primitive
279 erythropoiesis may pre-adapt *Astyanax* for colonizing hypoxic cave environments.
280 The expansion of erythropoiesis into the ALM during primitive hematopoiesis in
281 *Astyanax* contrasts strikingly to zebrafish, medaka, and other teleosts that have been investigated,
282 in which primitive erythropoiesis is confined to the PLM, and the ALM is devoted only to
283 myelopoiesis (Detrich et al., 1995; Govoni et al., 2005, Moriyama et al., 2010). Expression of
284 the macrophage marker *lcp1* (Herbomel et al., 2001) indicated that myelopoietic precursors had
285 already differentiated into macrophages as erythrocyte progenitors were being formed in the
286 ALM during early *Astyanax* development. Cell tracing studies have shown that blood precursor
287 cells can produce either erythrocytes or macrophages, but not both cell types (Warga et al.,
288 2009), indicating an opposing relationship between the erythroid and myeloid cell populations.
289 However, this relationship can be reversed by knockdown of the myeloid-controlling
290 transcription factor PU.1, which induces blood precursors of the ALM to form erythrocytes
291 instead of macrophages (Rhodes et al., 2005). Apparently, teleosts are potentially able to
292 undergo erythropoiesis in the ALM and PLM, but in most species this capacity is normally
293 confined to the PLM. In *Astyanax,* the balanced relationship between myeloid and erythroid cell
294 specification appears to have tilted toward the production of erythrocytes. However, the
295 development of erythrocytes in the ALM may not be at the expense of fewer myeloid cells
296 because there is also an overall expansion of the ALM (and PLM), which may promote the

297 specification of more blood precursor cells. In future studies, it will be interesting to determine
298 how the expansion of erythropoietic potential is controlled in cavefish.

299 Specification of cells in the primitive blood lineage can be traced to their positions during
300 gastrulation in zebrafish (Kimmel et al., 1990): ALM macrophages are originally derived from
301 progenitors on the dorsal side of the embryo, and PLM erythrocytes originate from the ventral
302 side of the embryo (Davidson and Zon, 2004; Warga et al., 2009). Erythrocyte progenitors
303 corresponding to the ALM and PLM are also likely to be positioned on the dorsal or ventral sides
304 respectively in gastrulating *Astyanax* embryos. Therefore, increased erythropoiesis in the ALM
305 suggests that a relative ventralization of hematopoietic development has evolved in cavefish
306 compared to surface fish. This possibility is supported by expanded erythroid development
307 induced by overexpression of the ventralizing factors *bmp2b* and *bmp7* in zebrafish gastrulae
308 (Lengerke et al., 2008) and is in line with evidence implicating the importance of maternal
309 factors in dorsal-ventral axis determination of cavefish embryos (Ren et al; 2018; Ma et al.,
310 2018; Torres-Paz et al., 2019). Maternal control of primitive erythropoiesis may promote
311 maximal oxygen distribution at the early stages of development in hypoxic environments. This
312 finding extends our understanding of evolutionary differences in early hematopoiesis to events
313 beginning during oogenesis.

314 In the present investigation, we have examined primitive hematopoiesis and red blood
315 cells in the Pachón cavefish population. About 30 different *Astyanax* cavefish populations have
316 been described in northeastern Mexico, and some of these cavefish are thought to have been
317 derived independently from surface fish ancestors (Gross, 2012; Herman et al., 2018). It is
318 conceivable that diverse cavefish lineages inhabit cave pools with different levels of
319 oxygenation. Therefore, in the future it would be interesting to determine the status of

320 erythrocytes in additional cavefish populations. It will also be important to determine if other
321 aquatic cave animals modify their oxygen delivery systems to cope with hypoxia.
322 Teleosts show considerable diversity in utilizing hemoglobin and red blood cells for
323 oxygen transport during development: some species begin hemoglobin synthesis during
324 embryogenesis, whereas others postpone hemoglobin and erythrocyte production until much
325 later in larval development (Wells, 2009). Our studies on the induction of hemolytic anemia
326 with PHZ confirm the functional significance of red blood cells produced during early *Astyanax*
327 development. At the same PHZ concentrations, surface fish, but not cavefish with residual red
328 blood cells, show negative effects on growth, and hypoxia treatment inhibited growth in surface
329 fish but not in cavefish. These results suggest that red blood cells are necessary for oxygen
330 transport at early stages of *A. mexicanus* development and that increased erythrocytes may be
331 advantageous in cavefish. This is contrary to zebrafish, where PHZ induced anemia showed that
332 red blood cells are not required during the first few weeks of development under normoxic
333 conditions (Pelster and Burggren, 1996), although under severe hypoxia zebrafish embryos also
334 use red blood cells to increase the supply of oxygen (Rombough and Drader, 2009).
335 Teleosts have evolved different strategies to cope with environments depleted in oxygen,
336 including changes in gill morphology (Sollid et al., 2003; Dhillon et al., 2013), behavioral
337 avoidance of hypoxic waters (Congleton, 1980; Mandic et al., 2009), and altered metabolism
338 (Torres et al., 2012). *Astyanax* surface fish larvae appear to deal with hypoxia by conserving
339 energy and reducing growth. It is likely that growth is regulated similarly to zebrafish via
340 upregulation of *igfbp1a* (Kajimura et al., 2005). The upregulation of *igfbp1* under hypoxia is
341 regulated by HIF1 (Kajimura et al., 2006). *Astyanax* cavefish, which are presumably unable to
342 avoid hypoxic waters in their natural environment, show increased expression of some of the *hif1*

343 genes in either hypoxic or normoxic conditions. The constitutive increase in *hif1* related gene
344 expression may have conferred growth resistance to hypoxia, even under conditions in which
345 *igfbp1* is upregulated, and may be responsible for increased red blood cell number.
346 The increased expression of the metabolic gene *hk1*in cavefish compared to surface fish
347 indicates an increase in glycolysis, consistent with the observations of Krishnan et al. (2019).
348 The increase in glycolysis does not seem to affect the TCA cycle since *ldha* and *pdk1* are not
349 differentially expressed between cavefish and surface fish (Medley et al., 2020). Wild captured
350 cavefish also have higher expression of the genes encoding enzymes involved in glutathione
351 metabolism compared to wild caught surface fish (Krishnan et al., 2019; Medley et al., 2020).
352 Glutathione is an important player in the mitigation of ROS, and the Pentose Phosphate Pathway
353 produces a large portion of the NADPH used in the production of glutathione (Stincone et al.,
354 2015). Therefore, the constitutive expression of *hif1*-genes in cavefish could play a role in ROS
355 mitigation via glutathione during hypoxia (Birnie-Gauvin et al., 2017).
356 In conclusion, the present investigation has revealed two potential adaptations that may
357 have permitted *Astyanax* cavefish to cope with hypoxic cave waters. First, cavefish have
358 enhanced erythrocyte development, and as a maternal effect this phenotype may have increased
359 the capacity of cavefish to carry and distribute essential oxygen to tissues and organs early in
360 development. Second, cavefish have adjusted to hypoxic conditions by evolving constitutively
361 high expression levels of some of the *hif1* genes. Together, these changes may be important for
362 the successful adaptation of *Astyanax* to hypoxic subterranean environments.
363
364 **Materials and methods**
365

Key Resources Table				
Reagent type (species) or resource	**Designation**	**Source or reference**	**Identifiers**	**Additional information**
gene (*Astyanax mexicanus* surface fish)	*hemoglobin subunit beta-2-like*, *hbb2*	NCBI:GeneID 111196758, Ensembl:ENSAMXG00000031275		
gene (*Astyanax mexicanus* surface fish)	*growth factor independent 1A transcription repressor a, gfi1aa*	NCBI:GeneID103029320 Ensembl:ENSAMXG00000006669		
gene (*Astyanax mexicanus* surface fish)	*LIM domain only 2 (rhombotin-like 1), lmo2*	NCBI:GeneID 111190647 Ensembl:ENSAMXG00000032986		
gene (*Astyanax mexicanus* surface fish)	*lymphocyte cytosolic protein, lcp1*	NCBI:GeneID 103042114 Ensembl:ENSAMXG00000012855		
gene (*Astyanax mexicanus* surface fish)	*hbbe2*	Ensembl:ENSAMXG00005017210		
gene (*Astyanax mexicanus* surface fish)	*ribosomal protein L13a, rpl13a*	NCBI:geneID: 103025160 Ensembl:ENSAMXG00000033532		
gene (*Astyanax mexicanus* surface fish)	*guanine nucleotide binding protein (G protein) beta polypeptide 1b, gnb1b*	NCBI:GeneID 103023031 Ensembl:ENSAMXG00000040710		

gene (*Astyanax mexicanus* surface fish)	*hypoxia inducible factor 1 subunit alpha a, hif1aa*	NCBI:GeneID 103022448 Ensembl:ENSAMXG00000039550		
gene (*Astyanax mexicanus* surface fish)	*hypoxia inducible factor 1 subunit alpha b, hif1ab*	NCBI:GeneID 103033873 Ensembl:ENSAMXG00000019342		
gene (*Astyanax mexicanus* surface fish)	*hypoxia inducible factor 1 subunit alpha like, hif1alike, hif1al*	NCBI:GeneID 103027586 Ensembl:ENSAMXG00000008564		
gene (*Astyanax mexicanus* surface fish)	*hypoxia inducible factor 1 subunit alpha like 2, hif1alike2, hif1al2*	NCBI:GeneID 103041845 Ensembl:ENSAMXG00000007272		
gene (*Astyanax mexicanus* surface fish)	*hexokinase 1, hk1*	NCBI:GeneID 103028521 Ensembl:ENSAMXG00000012670		
gene (*Astyanax mexicanus* surface fish)	*glucose-6-phosphate dehydrogenase, g6pd*	NCBI:GeneID 103035433 Ensembl:ENSAMXG00000017509		
gene (*Astyanax mexicanus* surface fish)	*lactate dehydrogenase A4, ldha*	NCBI:GeneID 103047177 Ensembl:ENSAMXG00000032467		
gene (*Astyanax mexicanus* surface fish)	*pyruvate dehydrogenase kinase 1, pdk1*	NCBI:GeneID 103033744 Ensembl:ENSAMXG00000039808		

gene (*Astyanax mexicanus* surface fish)	*insulin-like growth factor binding protein 1a, igfbp1a*	NCBI:GeneID 103033920 Ensembl:ENSAMXG00000009512		
strain, strain background (Escherichia coli)	One Shot Top10 chemically competent cells, *E.coli*	Invitrogen	Cat# 404003	
biological sample (*Astyanax mexicanus* surface fish)	Surface fish, SF, Texas	Jeffery lab		
biological sample (*Astyanax mexicanus* cave fish)	Cave fish, CF, Pachón,	Jeffery lab		
antibody	Anti-Dig-AP (sheep polyclonal)	Roche	Cat# 11093274910 RRID:AB_514497	(1:5000)
recombinant DNA reagent	pCRII-TOPO dual promotor vector	Invitrogen	Cat# 45-0640	
peptide, recombinant protein	Proteinase K	Roche	Cat# 03115887001	
peptide, recombinant protein	DNaseI I, RNase-free	Thermo-Scientific	Cat# EN0521	
commercial assay or kit	SYBR Premix Ex Taq (Tli RNaseH Plus)	Takara	Cat# RR420L	
commercial assay or kit	T7 RNA polymerase	Roche	Cat# 10881767001	
commercial assay or kit	SP6 RNA polymerase	Roche	Cat# 10810274001	

commercial assay or kit	ReadyMix Taq PCR Reaction Mix	Sigma	Cat# P4600	
commercial assay or kit	Dig RNA labelling Mix	Roche	Cat# 11277073910	
commercial assay or kit	Blocking reagent	Roche	Cat# 11096176001	
commercial assay or kit	BM Purple AP Substrate, precipitating	Roche	Cat# 11442074001	
commercial assay or kit	SuperScript III First strand synthesis supermix	Invitrogen	Cat# 18080-400	
commercial assay or kit	SuperScript IV VILO mastermix with ezDNase	Invitrogen	Cat# 11766050	
chemical compound, drug	paraformaldehyde	Electron Microscopy Sciences	Cat# 15710	
chemical compound, drug	o-dianisidine	Sigma	Cat# D9143	
chemical compound, drug	phenylhydrazine hydrochloride	Sigma	Cat# 114715	
chemical compound, drug	Trizol	Life Technologies	Cat# 15596018	

software, algorithm	Image-J	Imagj.nih.gov	RRID:SCR_003070	
software, algorithm	JMP Pro 14	SAS Institute Inc.		
other	CytoOne 24 well plate	USA Scientific	Cat# CC76727424	
other	Cellstar 12 well cell culture plate	Greiner	Cat# 665180	
other	Netwell inserts	Corning	Cat# 3478	
other	Hypoxia chamber, ProOx Model P110	BioSpherix		

366

367 *Biological materials*

368 *Astyanax mexicanus* surface fish and cavefish were obtained from laboratory stocks
369 descended from collections in Balmorhea Springs State Park, Texas and Cueva de El Pachón,
370 Tamaulipas, Mexico respectively. Fish were raised in a constant flow culture system as described
371 previously (Jeffery et. al. 2000; Ma et al., 2021). Embryos were obtained by natural spawning
372 and reared at 23°C. Fish handling and husbandry protocols were approved by the University of
373 Maryland Animal Care and Use Committee (IACUC #R-NOV-18-59) (Project 1241065-1) and
374 conformed to National Institutes of Health guidelines.

375

376 *Generation of reciprocal crosses*

377 The offspring of reciprocal crosses were generated by placing a female cavefish and a
378 male surface fish or a female surface fish and a male cavefish together in a tank and inducing
379 spawning by increased feeding and water temperature (Ma et al., 2021). Controls were generated
380 by crossing a surface fish male and surface fish female and a cavefish male and cavefish female.
381

382 *Quantification of circulating blood cells*

383 The number of circulating blood cells was analyzed in surface fish and cavefish larvae
384 immobilized by treatment with 2 μg ml^{-1} tricaine buffered with Tris to pH 7.0 (Western
385 Chemical, Inc, Ferndale, WA, USA) at 36 hrs. post-fertilization (hpf) and placed in water on a
386 concave microscope slide. Blood flow was imaged as cells flowed through the Duct of Cuvier
387 (Isogai, 2001) for 10 seconds using a stereoscope (Olympus SZX12) or a compound microscope
388 (Zeiss, Axioskop2) with 50x magnification and a 5 MP, Color, AmScope Microscope Eyepiece
389 Camera (MD500). Recordings were captured with Photobooth on a Macbook computer via USB
390 (OS 10.13.6). Videos were rendered into separate frames in Adobe Photoshop (CC2017, Adobe
391 Inc., San Jose, CA, USA) and processed and analyzed in Image-J (Schindelin et al.,
392 2012), (RRID:SCR_003070). After conversion to 32 bit, a data image showing the movement of
393 particles was created by subtracting two frames 0.15 seconds apart. This data image was used in
394 the plugin TrackMate (Tinevez et al., 2017) to analyze the number of moving blood cells in a
395 region of interest (ROI) covering 50% or more of the blood stream over the yolk (150x150
396 pixels). Using the LoG detector, moving blood cells were automatically detected by setting the
397 "blob diameter" to 5 and the threshold to 2. An automatic quality threshold was used to obtain

398 the number of circulating blood cells and checked against the recording for accuracy. The blood
399 flow of larvae from at least 8 different clutches of eggs per morph were analyzed.
400
401 *Staining and quantification of erythrocytes*
402 Red blood cells were stained at 36 hpf with 0.6 mg ml^{-1} o-dianisidine (Sigma-Aldrich, St.
403 Louis, MO, USA), 0.01 M sodium acetate (pH 4.5), 0.65 % H_2O_2 for 15 min in the dark (Iuchi
404 and Yamamoto, 1983). The stained embryos were rinsed in phosphate buffered saline (PBS),
405 fixed in 4% paraformaldehyde (PFA), and imaged as described below for *in situ* hybridization
406 50x magnification. The number of blood cells were counted manually in an ROI (150x150
407 pixels) by hand. Larvae from 3 separate clutches of eggs were used per morph.
408
409 *In situ hybridization*
410 *In sit*u hybridizations were performed using probes to the *hemoglobin subunit beta-2-like*
411 (*hbb2*), *growth factor independent 1A transcription repressor* (*gfi1aa*), *LIM domain only 2*
412 (*lmo2*), or *lymphocyte cytosolic protein 1* (*lcp1*) genes. Genes were cloned from a 24 hpf surface
413 fish cDNA library and 10 hpf, 24 hpf and 30 hpf cavefish cDNA libraries using the pCRII TOPO
414 dual promoter vector (ThermoFisher Scientific, Waltham, MA, USA) transformed into One shot
415 Top10 cells and the following primers: *hbb2* (24 hpf SF; ENSAMXG00000031275: 5'-
416 gcaggacaagtagaaacctcaaagtc-3' and 5'-tttcgtaagggcagagcctaca-3'), *gfi1aa* (24 hpf CF;
417 ENSAMXG00000006669:5'-gaaggtctgcgctcgtgatatt-3' and 5'- agttatccgcggtgtgaacag-3'), *lmo2*
418 (10 hpf CF; ENSAMXG00000032986: 5'-ggcctctacaatcgagaggaaa-3' and 5'
419 taccaagttgccgtttagtttgg-3'), and *lcp1* (36 hpf CF; ENSAMXG00000012855: 5'-
420 aggccttcagcaaagttgatgtg-3' and 5'-ttcaggtcctctgcaccgatatt-3'). DIG labeled probes were made

421 using SP6 or T7 transcription kits (Roche, Mannheim, Germany) from linearized plasmid or, in
422 the case of *gfi1aa,* from a PCR product made with the cloned cDNA as template and the above
423 mentioned primers, after a RNA-polymerase promoter site was added to the 5' end.
424 *In situ* hybridizations were performed as previously described (Ma et al., 2014). Briefly,
425 stored (-20°C) 4% PFA fixed and methanol dehydrated embryos were rehydrated stepwise into
426 PBS, fixed with 4% PFA, digested with proteinase K, fixed with 4% PFA, and hybridized with
427 probes at 60°C for 16 hours. Un-hybridized probe was removed by 2 X and 0.2 X SSCT (150
428 mM sodium chloride; 15 mM sodium citrate; 0.1% Tween 2) stringency washes followed by
429 incubation in MABT blocking solution (Roche) and subsequently with anti-DIG-AP Fab
430 fragments (Roche), (RRID:AB_514497). Embryos were rinsed in MABT buffer and PBS,
431 equilibrated in AP buffer, and stained with BM-Purple (Roche). The stained embryos were
432 imaged and photographed using a Zeiss Discovery V20 stereoscope with a Zeiss AxioCam HRc
433 camera.
434
435 *Induction of hemolytic anemia with phenylhydrazine*
436 Phenylhydrazine hydrochloride (PHZ; Sigma-Aldrich, St. Louis, MO, USA) was used to
437 induce hemolytic anemia (Houston et al., 1988). At 14 hpf, 20 manually de-chorionated embryos
438 were placed in clean fish system-water containing a particular concentration of PHZ or clean fish
439 system water as a control. Embryos were incubated with PHZ for 28 hours when blood
440 circulation was clearly visible over the yolk. Embryos were fixed and used for *in situ*
441 hybridization with a *hbb2* probe. In a separate experiment, embryos were imaged on a Zeiss
442 Axioskop2 microscope with a Axiocam 503 camera and measurements of tail length (the axial
443 length from the posterior end of the yolk mass to the tip of the tail) were made in Image-J. After

444 imaging, PHZ treated embryos and controls were stained with o-dianisidine and imaged for
445 blood cell quantification as described above. Because low numbers of blood cells were present
446 after PHZ treatment, blood cells were counted in a larger area covering the whole anterior side of
447 the yolk in lateral view (400 pixels wide). Larvae of two separate clutches of eggs were used per
448 morph for the latter experiment.

449 Surface fish larvae were also treated with PHZ at 34 hpf for 1 hr., rinsed extensively for 1
450 hr., imaged with a microscope as described above, and left for 16 hrs. before imaging again. At
451 the end of the experiment, larvae were stained with o-dianisidine. The length of the post-anal tail
452 was measured using Image-J and growth determined as the differential between the two time
453 points. Blood cell number was determined by manual counting as described above.

454

455 *Laboratory hypoxia treatment and growth determinations*

456 A hypoxia chamber (ProOx Model P110, BioSpherix, Parish, NY, USA) was used to
457 create a hypoxic laboratory environment in which oxygen was reduced by nitrogen gas (HP,
458 Airgas, Hyattsville, MD, USA). At 30 hpf larvae were exposed to hypoxia (1 mg/L oxygen) for
459 18 hours or to normoxia (outside of the chamber). Larvae were placed individually in wells of a
460 24 well plate (CytoOne, USA scientific, Ocala, FL, USA) containing 2 ml clean fish system-
461 water. Twenty-four larvae were used per treatment for surface fish and 48 larvae for cavefish
462 from two separate clutches of eggs per morph. To measure post-anal tail growth, each larva was
463 imaged before placement in a well and again at the end of the treatment using a microscope as
464 described above. Image-J was used to measure post-anal tail length (Fig. 6A) and growth
465 determined as the differential between the two time points. To measure eye size, eye diameter
466 was measured after the 18 hr. hypoxia or normoxia treatment with image -J. After imaging,

467 larvae were stained with o-dianisidine and blood cells were counted from images as described
468 above.
469
470 *RNA isolation and quantitative real time polymerase chain reactions*
471 To compare the extent of early erythropoiesis between cavefish and surface fish, the
472 expression of *hemoglobin beta embryonic 2* (*hbb2*) and *hbbe2*, (*hbbe2* encodes an *A. mexicanus*
473 embryonic β-hemoglobin most similar to zebrafish *hbbe1*; Ganis et al., 2012) genes and the
474 *gfi1aa* gene were quantified at 10, 24 and 60 hpf. Three potential reference genes were
475 evaluated: *ribosomal protein L13a* (*rpl13a*), *actin alpha 1* (*acta1b*), and *lsm12a.* Only *rpl13a*
476 did not vary over time or between surface and cavefish and was therefore used as the final
477 reference gene. RNA was extracted from 30 embryos with Trizol (ThermoFisher), treated with
478 RNase-free DNase I (ThermoFisher), cleaned and concentrated by phenol/chloroform extraction
479 and precipitated with ammonium acetate and ethanol. Poly(A)-primed cDNA was made with
480 SuperScript III First Strand Synthesis SuperMix (ThermoFisher) and used in qPCR with Takara
481 SYBR Premix Ex Taq (Tli RNaseH Plus) (Takara Bio USA Inc., Mountain View, CA, USA) and
482 LC480 (Roche).
483 In the laboratory hypoxia experiments, RNA was isolated from 24 larvae placed in the 15
484 mm Netwell insert (Corning, Corning, New York, USA) in a well of a 12 well plate. Two hours
485 after the start of the hypoxia treatment the larvae were collected in Trizol (ThermoFisher) within
486 1 min after taking them out the hypoxia chamber by removing the Netwell inserts from the wells,
487 decanting excess water, and the larvae were immersed in Trizol. RNA was isolated for 6 samples
488 of 24 larvae each with 3 samples per clutch of eggs. Two separate clutches of eggs were used per
489 morph.

490 The amounts of *hypoxia inducible factor 1*(*hif1aa*) and its duplicate gene *hif1ab*, *hypoxia*
491 *inducible factor 1-like* (*hif1alike*) and its duplicate gene *hif1alike2* (equivalent to *hif3a*), *insulin*
492 *growth factor binding protein 1a* (*igfbp1a*), *hexokinase 1* (*hk1*), *glucose-6-phosphate*
493 *dehydrogenase* (*G6PD*), *lactate dehydrogenase a* (*ldha*) and *pyruvate dehydrogenase kinase 1*
494 (*pdk1*) were quantified by qPCR in surface fish and cavefish larvae exposed to hypoxic or
495 normoxic conditions. We evaluated *rpl13a*, *acta1b*, *endoplasmic reticulum protein 44* (*erp44*)
496 and *guanine nucleotide binding protein ß polypeptide 1b* (*gnb1b*) as potential reference genes:
497 *gnb1b* had Ct values closest to the Ct values of the queried genes, did not differ between
498 normoxic and hypoxic surface fish or cavefish, and was chosen as a reference gene. RNA was
499 extracted from 24 embryos and treated with ezDNase and cDNA was made with SuperScript IV
500 VILO mastermix (ThermoFisher). The primers used in qPCR analysis are shown in Table 2.
501 A ΔCt for each gene was calculated by subtracting the average Ct value of each reference
502 gene. For comparison of gene expression in cavefish to surface fish over time, ΔΔCt was
503 calculated by subtracting the average ΔCt of surface fish at 10 hpf from each ΔCt for each gene.
504 For comparison of gene expression under normoxic and hypoxic conditions, the ΔCt of surface
505 fish under normoxic conditions was subtracted from the ΔCt for each gene. For graphical
506 representation, the fold change was calculated as $2^{-(\Delta\Delta Ct)}$, where values >1 show an increase and
507 values <1 a decrease. Variation was expressed as the range of fold change $2^{-(\Delta\Delta Ct+stdev_{\Delta\Delta Ct})}$ for the
508 upper value or $2^{-(\Delta\Delta Ct-stdev_{\Delta\Delta Ct})}$ for the lowest value.
509
510 *Statistics*
511 Statistics were done using JMP pro 14 (SAS Institute Inc.). Normal distribution of data
512 was determined using the Shapiro Wilk test. Comparison of blood cell number was done using

513 Wilcoxon/Kruskal-Wallis Rank Sums test (1F N = 72, 1G N=36) ($p < 0.05$). Expression as ΔΔCt
514 of *hbb2, hbbe2* and *gfi1aa* over time was analyzed per gene with a two-way ANOVA followed
515 by pairwise comparison with Student's t-test (*hbb2* N=8, *hbbe2* N=4, *gfi1aa* N=3), ($p<0.05$).
516 Comparisons of blood cell number in reciprocal hybridization experiments were analyzed using a
517 Wilcoxon/Kruskal-Wallis Rank Sums test followed by Wilcoxon for each pair (N=20), ($p<0.05$).
518 Differences in tail length between surface and cavefish at different concentrations of PHZ were
519 analyzed using Wilcoxon/Kruskal-Wallis Rank Sums test followed by Wilcoxon for surface fish
520 (SF) or cavefish (CF) for each pair (SF 0, 2 mg L^{-1} N=23, SF 1, 3 mg L^{-1} N=24, CF 0, 1, 2 mg L^{-}
521 ^{1} N=24, CF 3 mg L^{-1}), ($p<0.05$). Comparison of blood cell number at different concentrations of
522 PHZ were analyzed with Wilcoxon/Kruskal-Wallis Rank Sums test followed by Wilcoxon for
523 each pair (SF 0, 1, 2 and CF 3 mg L^{-1} N=20, SF 3 mg L^{-1} N=10, CF 0 mg L^{-1} N=19, CF 1 mg L^{-1}
524 N=21, CF 2 mg L^{-1} N=22), ($p<0.05$). Post-anal tail growth at 0 and 5 mg L^{-1} PHZ was analyzed
525 with a Student's t-test (0 mg L^{-1} N=19, 5 mg L^{-1} N=20), ($p<0.05$) and cell number with
526 Wilcoxon/Kruskal-Wallis Rank Sums test (N=10), ($p<0.05$). Post-anal tail growth under
527 normoxic and hypoxic conditions was analyzed with Wilcoxon/Kruskal-Wallis Rank Sums test
528 followed by Wilcoxon for each SF and CF pair (SF-N and SF-H N=23, CF-N N=46 and CF-H
529 N=47), ($p<0.05$). Cell number under normoxic and hypoxic conditions was analyzed with one-
530 way ANOVA followed by Student's t-test (SF-N N=22, SF-H N=21, CF-N N=47, CF-H N=45),
531 ($p<0.05$). The diameter of eye was analyzed by one-way ANOVA followed by Student's t-test
532 (SF-N N=18, SF-H N=14, CF-N N=30, CF-H N=28), ($p<0.05$). Expression as ΔΔCt of genes
533 under normoxic and hypoxic conditions was analyzed per gene by one-way ANOVA followed
534 by Student's t-test or when variances where unequal with Wilcoxon/Kruskal-Wallis Rank Sums
535 test followed by Wilcoxon for each pair (N = 6), ($p<0.05$).

536

537 **Acknowledgments**

538

539 This research was supported by NIH grant EY024941 to WRJ. We thank Ruby
540 Dessiatoun and Karina Lacroix for maintenance of the *A. mexicanus* colony and Mandy Ng for
541 technical assistance.

542

543 **Competing interests**

544

545 The authors declare no competing or financial interests

546 **Funding**

547

548 Funding for this study was provided by the National Institutes of Health (EY024941 to
549 WRJ)

550

551 **References**

552

553 **Aspiras AC, Rohner N, Martineau B, Borowsky RL, Tabin CJ.** 2015. Melanocortin 4
554 receptor mutations contribute to the adaptation of cavefish to nutrient-poor conditions.
555 *Proceedings of the National Academy of Sciences of the United Stated of America* **112**: 9668-
556 9673. doi:10.1073/pnas.1510802112

557

558 **Birnie-Gauvin K, Costantini D, Cooke SJ, Willmore WG.** 2017. A comparative and

559 evolutionary approach to oxidative stress in fish: A review. *Fish and Fisheries* **18**:928-942.
560 doi.org/10.1111.faf.12215.
561
562 **Bishop RE, Kakuk B, Torres JJ.** 2004. Metabolism and proximate composition of Caribbean
563 troglobitic crustaceans with observations on the water chemistry of two anchialine caves.
564 *Journal of Crustacean Biology*. **24**:379-392. https://doi.org/10.1651/C-2459
565
566 **Blin M, Tine E, Meister L, Elipot Y, Bibliowicz J, Espinasa L, Rétaux, S.** 2018**.**
567 Developmental evolution and developmental plasticity of the olfactory epithelium and olfactory
568 skills in Mexican cavefish. *Developmental Biology* **441**:242-251**.**
569
570 **Boggs T, Gross J.** 2021. Reduced oxygen as an environmental pressure in the evolution of the
571 blind Mexican cavefish. *Diversity* **13**:26. doi.org/10.3390/d13010026
572
573 **Brownlie A, Hersey C, Oates AC, Paw BH, Falick AM, Witkowska HE, Flint J, Higgs D,**
574 **Jessen J, Bahary N, Zhu H, Lin S, Zon L.** 2003. Characterization of embryonic globin genes of
575 the zebrafish. *Developmental Biology*. **255**:48-61. doi: 10.1016/s0012-1606(02)00041-6
576
577 **Cai X, Zhou Z, Zhu J, Liao Q, Zhang D, Liu X, Wang J, Ouyang G, Xiao W.** 2020.
578 Zebrafish Hif3α modulates erythropoiesis via regulation of gata1 to facilitate hypoxia tolerance.
579 *Development.* **147**: dev185116. doi: 10.1242/dev.185116.
580
581 **Carroll KJ, North TE.** 2014.. Oceans of opportunity: exploring vertebrate hematopoiesis in

582 zebrafish. *Experimental Hematology*. **42**:684-696. doi:10.1016/j.exphem.2014.05.002

583

584 **Congleton JL**. 1980. Observations on the responses of some southern California tide pool fishes

585 to nocturnal hypoxic stress. *Comparative Biochemical Physiology*. **66A**:719-122.

586 https://doi.org/10.1016/0300-9629(80)90026-2

587

588 **Cooney J D, Hildick-Smith GJ, Shafizadeh E, McBride PF, Carroll KJ, Anderson H, Shaw**

589 **GC, Tamplin OJ, Branco DS, Dalton AJ, Shah DI, Wong C, Gallagher PG, Zon LI, North**

590 **TE, Paw BH.** 2013. Teleost *growth factor independence* (*gfi*) genes differentially regulate

591 successive waves of hematopoiesis. *Developmental Biology* 373:431-441. doi:

592 10.1016/j.ydbio.2012.08.015

593

594 **Cui XG, Han ZT, He SH, Wu XD, Chen TR, Shao CH, Chen DL, Su N, Chen YM, Wang T,**

595 **Wang J, Song D-W, Yan W-J, Yang X-H, Liu T, Wei H-F, Xiao J.** 2017. HIF1/2α mediates

596 hypoxia-induced LDHA expression in human pancreatic cancer cells. *Oncotarget* 8:24840-

597 24852. doi:10.18632/oncotarget.15266.

598

599 **Culver DC, Pipan T**. 2009. *The Biology of Caves and Other Subterranean Habitats.* Oxford

600 UK: Oxford University Press.

601

602 **Davidson AJ, Zon LI.** 2004. The 'definitive' (and 'primitive') guide to zebrafish hematopoiesis.

603 *Oncogene* **23**:7233-7246. doi: 10.1038/sj.onc.1207943.

604

605 **Detrich HW, Kieran M W, Chan FY, Barone LM, Yee K, Rundstadler J, Pratt S, Ransom**
606 **D, Zon LI.** 1995. Intraembryonic hematopoietic cell migration during vertebrate development.
607 *Proceedings of the National Academy of Sciences of the United States of America* **92**:10713-
608 10717. doi: 10.1073/pnas.92.23.10713
609
610 **Dhillon RS, Yao L, Matey V, Chen B-J, Zhang A-J, Cao Z-D, Fu S-J, Brauner CJ, Wang**
611 **YS, Richards JG.** 2013. Interspecific differences in hypoxia-induced gill remodeling in carp.
612 *Physiology Biochemisty Zoology* 86:727-739. doi: 10.1086/673180
613
614 **Fumey J, Hinaux H, Noirot C, Thermes C, Rétaux S, Casane D**. 2018. Evidence for late
615 Pleistocene origin of *Astyanax mexicanus* cavefish. *BioMed Central Evolutionary Biology.*
616 **18(1)**:43. doi: 10.1186/s12862-018-1156-7.
617
618 **Ganis J J, Hsia N, Trompouki E, de Jong JLO, DiBiase A, Lambert J S, Zhiying J, Sabo**
619 **PJ, Weaver M, Sandstrom R, Stamatoyannopoulos JA, Zhou Y, Zon LI.** 2012. Zebrafish
620 globin switching occurs in two developmental stages and is controlled by the LCR.
621 *Developmental Biology* **366**:185-194. doi: 10.1016/j.ydbio.2012.03.021
622
623 **Gering M, Yamada Y, Rabbitts TH, Patient RK.** 2003. Lmo2 and Scl/Tal1 convert non-axial
624 mesoderm into haemangioblasts which differentiate into endothelial cells in the absence of
625 Gata1. *Development* **130**:6187-6199. doi:10.1242/dev.00875
626
627 **Giaccia A J, Simon MC, Johnson R.** 2004. The biology of hypoxia: the role of oxygen
628 sensing in development, normal function, and disease. *Genes & De*velopment **18**: 2183-2194.

Gore AV, Pillay L M, Galanternik MV, Weinstein BM. 2018. The zebrafish: A fintastic model for hematopoietic development and disease. *Wiley Interdisciplinary Reviews in Developmental Biology* **7**:e312-328. doi: 10.1002/wdev.312.

Govoni JJ, West MA, Bonaventura J, Goddette G, Jenkins TE. 2005. The ontogeny of hematopoiesis in the marine teleost *Leiostomus xanthurus* and a comparison of the site of initial hematopoiesis with *Opsanus tau*. *Journal of Fish Biology*. **67**:696-712. https://doi.org/10.1111/j.0022-1112.2005.00770.x

Gross JB. 2012. The complex origin of *Astyanax* cavefish. *BioMed Central Evolutionary Biology*. **12**:105-116. doi: 10.1186/1471-2148-12-105.

Haase VH. 2013**.** Regulation of erythropoiesis by hypoxia-inducible factors. *Blood Review* **27**:41-53**.** doi: 10.1016/j.blre.2012.12.003

Herbomel P, Thisse B, Thisse C. 1999. Ontogeny and behaviour of early macrophages in the zebrafish embryo. *Development* **126**:3735-3745.

Herbomel P, Thisse B, Thisse C. 2001. Zebrafish early macrophages colonize cephalic mesenchyme and developing brain, retina and epidermis through a M-CSF receptor-dependent invasive process. *Develomental Biology*. **238**:274-288. doi: 10.1006/dbio.2001.0393

652 **Herman A, Brandvain Y, Weagley J, Jeffery WR, Keene AC, Kono TJY, Bilandžija H,**
653 **Borowsky R, Espinasa L, O'Quin K, Ornelas-García CP, Yoshizawa M, Carlson B,**
654 **Maldonado E, Gross JB, Cartwright RA, Rohner N, Warren WC, McGaugh SE.** 2018. The
655 role of gene flow in rapid and repeated evolution of cave related traits in Mexican tetra, *Astyanax*
656 *mexicanus*. *Molecular Ecology* **27**: 4397-4416. doi: 10.1111/mec.14877
657
658 **Houston AH, Murad A, Gray JD.** 1988. Induction of anemia in goldfish, *Carassius auratus* L.,
659 by immersion in phenylhydrazine hydrochloride. *Canadian Journal of Zoolo*gy **66**:729-
660 736. https://doi.org/10.1139/z88-108.
661
662 **Hüppop K.** 1986. Oxygen consumption of *Astyanax fasciatus* (Characidae, Pisces): a
663 comparison of epigean and hypogean populations. *Environmental Biology of Fishes* **17**: 299-308.
664
665 **Isogai S, Horiguchi M, Weinstein BM.** 2001. The vascular anatomy of the developing
666 zebrafish: an atlas of embryonic and early larval development. *Developmental Biology* 230: 278-
667 301. doi: 10.1006/dbio.2000.9995
668
669 **Iuchi I, Yamamoto M.** 1983. Erythropoiesis in the developing rainbow trout, *Salmo gairdneri*
670 *irideus*: histochemical and immunochemical detection of erythropoietic organs. *Journal of*
671 *Experimental Zoology*. **226**:409-417. doi: 10.1002/jez.1402260311
672
673 **Jeffery WR, Strickler A., Guiney S, Heyser D, Tomarev SI.** 2000**.** *Prox 1* in eye degeneration
674 and sensory compensation during development and evolution of the cavefish *Astyanax*.

675 *Development Genes & Evolution*. **210**:223-230**.** doi:10.1007/s004270050308.

676

677 **Kajimura S, Aida K, Duan C.** 2005. Insulin-like growth factor-binding protein-1 (IGFBP-1)
678 mediates hypoxia-induced embryonic growth and developmental retardation. *Proceedings of the*
679 *National Academy of Science of the United States of America* **102**: 1240-1245. doi:
680 10.1073/pnas.0407443102.

681

682 **Kajimura S, Aida K, Duan C.** 2006. Understanding hypoxia-induced gene expression in early
683 development: in vitro and in vivo analysis of hypoxia-inducible factor 1-regulated zebra fish
684 insulin-like growth factor binding protein 1 gene expression. *Molecular Cell Biology.* **26:**1142-
685 1155. doi: 10.1128/MCB.26.3.1142-1155.2006

686

687 **Kamei H.** 2020. Oxygen and embryonic growth: the role of insulin-like growth factor signaling.
688 *General & Comparative Endocrinology.* **294**:113473. doi: 10.1016/j.ygcen.2020.113473.

689

690 **Kimmel CB, Warga RM, Schilling TF.** 1990. Origin and organization of the zebrafish fate
691 map. *Development* **108**:581-594.

692

693 **Krishnan J, Persons JL, Peuß R, Hassan H, Kenzior A, Xiong S, Olsen L, Maldonado E,**
694 **Kowalko JE., Rohner N.** 2019. Comparative transcriptome analysis of wild and lab populations
695 of *Astyanax mexicanus* uncovers differential effects of environment and morphotype on gene
696 expression. *Journal of Experimental Zoology B. Molecular & Developmental Evolution* **334**:530-
697 539. doi: 10.1002/jez.b.22933

Kulkarni RP, Tohari S, Ho A, Brenner S, Venkatesh B. 2010. Characterization of a hypoxia-response element in the *Epo* locus of the pufferfish, *Takifugu rubripes*. Marine Genomics **3**:63-70. doi: 10.1016/j.margen.2010.05.001.

Le Guyader D, Redd MJ, Colucci-Guyon E, Murayama E, Kissa K, Briolat V, Mordelet E, Zapata A, Shinomiya H, Herbomel P. 2008. Origins and unconventional behavior of neutrophils in developing zebrafish. *Blood* **111**:132-141. doi: 10.1182/blood-2007-06-095398

Lengerke C, Schmitt S, Bowman TV, Jang I. H., Maouche-Chretien L, McKinney-Freeman, S, Davidson, AJ, Hammerschmidt M, Rentzsch F, Green JB, Zon L, et al.. 2008. BMP and Wnt specify hematopoietic fate by activation of the Cdx-Hox pathway. *Cell Stem Cell* **2**:72–82. doi:10.1016/j.stem.2007.10.022

Ma L, Parkhurst A, Jeffery W R. 2014. The role of a lens survival pathway including *sox2* and αA-crystallin in the evolution of cavefish eye degeneration. *Evo Devo*. **5**: 28-41. doi: 10.1186/2041-9139-5-28

Ma L, Strickler AG, Parkhurst A, Yoshizawa M, Shi J, Jeffery WR. 2018. Maternal genetic effects in *Astyanax* cavefish development. *Developmental Biology.* **441**:209-220. doi: 10.1016/j.ydbio.2018.07.014

720 **Ma L, Dessiatoun R, Shi J, Jeffery WR.** 2021. Incremental Temperature Changes for Maximal
721 Breeding and Spawning in *Astyanax mexicanus. The Journal of Visualized Experiments*
722 doi: 10.3791/61708
723
724 **Majmundar A J, Wong WJ, Simon MC**. 2010. Hypoxia-inducible factors and the response to
725 hypoxic stress. *Molecular Cell* **40**:294-309. doi:10.1016/j.molcel.2010.09.022
726
727 **Malard F, Hervant F** 1999. Oxygen supply and the adaptations of animals in groundwater.
728 *Freshwater Biology* **41**:1-30. https://doi.org/10.1046/j.1365-2427.1999.00379.x
729
730 **Mandic M, Sloman KA, Richards JG.** 2009. Escaping to the surface: A phylogenetically
731 independent analysis of hypoxia-induced respiratory behaviors in Sculpins. *Physiology*
732 *Biochemistry Zoology*. **82**, 730-738. doi: 10.1086/605932
733
734 **Mandic M., Joyce, W., Perry, S. F**. 2021. The evolutionary and physiological significance of
735 the Hif pathway in teleost fishes. *Journal of Experimental Biology* **224**, jeb231936.
736 Doi:10:1242/jeb.231936
737
738 **Martinez ML, Chapman LJ, Grady JM, Rees BB.** 2004. Interdemic variation in heamatocrit
739 and lactate dehydrogenase in the African cyprinid *Barbus neumayeri. Journal of Fish Biology.*
740 **65**:1056-1069.
741
742 **Medley JK, Person J, Peuß R, Olsen L, Xiong S, Rohner N.** 2020. Untargeted metabolomics

743 of the cavefish *Astyanax mexicanus* reveals the basis of metabolic strategies in adaptation to
744 extreme conditions**.** *BioRxiv* DOI: https://doi.org/10.1101/2020.10.27.358077
745
746 **Mitchell RW, Russel WH, Elliott WR.** 1977. *Mexican eyeless characin fishes, genus*
747 *Astyanax: environment, distribution and evolution*. (Lubbock: Texas Tech Press).
748
749 **Moore C, Richens J., Hough Y, Ucanok D, Malla S, Sang F, Chen Y, Elworthy S.**
750 **Wilkinson RN, Gering M.** 2018. Gfi1aa and Gfi1b set the pace for primitive erythroblast
751 differentiation from hemangioblasts in the zebrafish embryo. *Blood A*dvances **2**: 2589-2606. doi:
752 10.1182/bloodadvances.2018020156
753
754 **Moran D, Softley R, Warrant E J.** 2014**.** Eyeless Mexican cavefish save energy by eliminating
755 the circadian rhythm in metabolism**.** *Public Library of Science ONE* **9**:
756 e107877.https://doi.org/10.1371/journal.pone.0107877
757
758 **Moran D, Softley R. Warrant EJ.** 2015. The energetic cost of vision and the evolution of
759 eyeless Mexican cavefish. *Scientific Advances* **1**:e1500363. doi:10.1126/sciadv.1500363
760
761 **Moriyama A, Inohaya K, Maruyama K, Kudo A.** 2010. Bef medaka mutant reveals the
762 essential role of c-myb in both primitive and definitive hematopoiesis. *Developmental Biology*
763 **345**:133-143. doi: 10.1016/j.ydbio.2010.06.031
764
765 **Möröy T, Vassen L, Wilkes B, Khandanpour C.** 2015. From cytopenia to leukemia: the role

766 of Gfi1 and Gfi1b in blood formation. *Blood* **126**:2561-2569. doi:10.1182/blood-2015-06-
767 655043
768
769 **Ornelas-García P, Pajares S, Sosa-Jiménez VM, Rétaux S, Miranda-Gamboa RA.** 2018.
770 Microbiome differences between river-dwelling and cave-adapted populations of the fish
771 *Astyanax mexicanus* (De Filippi, 1853). *Peer Journal* **6**: e5906-5926. doi: 10.7717/peerj.5906
772
773 **Paik E J, Zon LI.** 2010. Hematopoietic development in the zebrafish. *International Journal of*
774 *Developmental Biology* **54:**1127-1137. doi: 10.1387/ijdb.093042ep.
775
776 **Patterson LJ, Gering M, Eckfeldt CE, Green AR, Verfaillie CM, Ekker SC, Patient R.**
777 2007. The transcription factors Scl and Lmo2 act together during development of the
778 hemangioblast in zebrafish. *Blood* **109**:2389-2398. doi:10.1182/blood-2006-02-003087
779
780 **Pelster B, Burggren WW.** 1996. Disruption of hemoglobin oxygen transport does not impact
781 oxygen-dependent physiological processes in developing embryos of zebra fish (*Danio rerio*).
782 *Circulation Research*. **7**:358-362. doi:10.1161/01.res.79.2.358
783
784 **Pelster B, Egg M.** 2018. Hypoxia-inducible transcription factors in fish: expression, function
785 and interconnection with the circadian clock. *Journal of Experimental Biology.* **221**:jeb163709.
786 doi: 10.1242/jeb.163709
787

Peuß R, Box AC, Chen S, Wang, Y, Tsuchiya D, Persons JL, Kenzior A, Maldonado E, Krishnan J, Scharsack JP, Slaughter B, Rohner N. 2020. Adaptation to low parasite abundance affects immune investment and immunopathological responses of cavefish. *Nature Ecology Evolution* **4,** 1416–1430 https://doi.org/10.1038/s41559-020-1234-2

Rashid I, Nagpure NS, Srivastava P, Kumar R, Pathak AK, Singh M, Kushwaha B. 2017. HRGFish: A database of hypoxia responsive genes in fishes. *Scientific Reports* **7**:42346. Doi: 10.1038/srep42346.

Ren X, Hamilton N, Müller F, Yamamoto Y. 2018. Cellular rearrangement of the prechordal plate contributes to eye degeneration in the cavefish. *Developmental Biol*ogy **441**:221-234. doi: 10.1016/j.ydbio.2018.07.017

Rhodes J, Hagen A, Hsu K, Deng M, Ting XL, Look T, Kanki JP. 2005**.** Interplay of Pu.1 and gata1 determines myelo-erythroid progenitor cell fate in zebrafish. *Developmental. Cell* **8**:97-108**.** doi: 10.1016/j.devcel.2004.11.014

Rohner N, Jarosz DF, Kowalko JE, Yoshizawa M, Jeffery WR, Borowsky RL, Lindquist S, Tabin CJ. 2013. Cryptic variation in morphological evolution: HSP90 as a capacitor for loss of eyes in cavefish. *Science* **342**:1372-1375. doi:10.1126/science.1240276.

Rombough R, Drader H. 2009. Hemoglobin enhances oxygen uptake in larval zebrafish (*Danio rerio*) but only under conditions of extreme hypoxia. *Journal of Experimental Biology* **212**:778-

811 784. doi: 10.1242/jeb.026575

812

813 **Rutjes HA, Nieveen MC, Weber RE, Witte F, Van den Thillart GEEJM.** 2007. Multiple
814 strategies of Lake Victoria cichlids to cope with lifelong hypoxia include hemoglobin switching.
815 *American Journal of Physiology. Regulatory, Integrative and Comparative. Physiology* **293**:
816 R1376-R1383. doi: 10.1152/ajpregu.00536.2006

817

818 **Sears CR, Boggs TE, Gross JB**. 2020. Dark-rearing uncovers novel gene expression patterns in
819 an obligate cave-dwelling fish. *Journal of Experimental Zoology Part B Molecular Development*
820 *Evolution.* **334**:518–529.

821

822 **Schindelin J, Arganda-Carreras I, Frise E, Kaynig V, Longair M, Pietzsch T, Preibisch S,**
823 **Rueden C, Saalfeld S, Schmid B, Tinevez J-Y, White DJ, Hartenstein V, Eliceiri K,**
824 **Tomancak P, Cardona A.** 2012. Fiji: an open-source platform for biological-image analysis.
825 *Nature Meth*ods **9**:676-682. 10.1038/nmeth.2019

826

827 **Semenza GL, Wang GL.** 1992. A nuclear factor induced by hypoxia via de novo protein
828 synthesis binds to the human erythropoietin gene enhancer at a site required for transcriptional
829 activation. *Molecular Cell Biology* **12**:5447-54. doi: 10.1128/mcb.12.12.5447

830

831 **Singh D, Arora R, Kaur P, Singh B, Mannan R, Arora S.** 2017. Overexpression of hypoxia-
832 inducible factor and metabolic pathways: possible targets of cancer. *Cell Bioscience.* **7**: 62. doi:
833 10.1186/s13578-017-0190-2

834

835 **Stincone A, Prigione A, Cramer T, Wamelink MMC, Campbell K, Cheung E, Olin-**
836 **Sandoval V, Grüning N-M, Krüger A, Alam MT, Keller MA, Breitenbach M, Brindle K,**
837 **Rabinowitz JD, Ralser M.** 2015. The return of metabolism: biochemistry and physiology of the
838 pentose phosphate pathway. *Biological Reviews of the Cambridge Philosophical Society* **90**:927-
839 963. doi: 10.1111/brv.12140.

840

841 **Sollid J, De Angelis P, Gundersen K, Nilsson GE.** 2003. Hypoxia induces adaptive and
842 reversible gross morphological changes in crucian carp gills. *Journal of Experimental Biology*
843 **206**:3667-3673. doi: 10.1242/jeb.00594

844

845 **Torres-Paz J, Leclercq J, Rétaux S.** 2019. Maternally regulated gastrulation as a source of
846 variation contributing to cavefish forebrain evolution. *eLIFE* **8**:e50160. doi:
847 https://doi.org/10.7554/eLife.50160

848

849 **Timmerman CM, Chapman LJ** 2004. Behavioral and physiological compensation for chronic
850 hypoxia in the sailfin molly (*Poecilia latipinna*). *Physiological Biochemical Zoology* **7**:601-610.
851 doi: 10.1086/421754

852

853 **Tinevez J-Y, Perry N, Schindelin J, Hoopes GM, Reynolds GD, Laplantine E, Bednarek**
854 **SY, Shorte SL, Eliceiri KW.** 2017. TrackMate: An open and extensible platform for single-
855 particle tracking. *Methods* **115**:80-90. doi:10.1016/j.ymeth.2016.09.016.

856

857 **Torres JJ, Grigsby MD, Clarke ME.** 2012. Aerobic and anaerobic metabolism in oxygen
858 minimum layer fishes: the role of alcohol dehydrogenase. *Journal of Experimental Biology*
859 **215**:1905-1914. doi:10.1242/jeb.060236
860
861 **Varatharasan N, Croll RP, Franz-Odendaal T.** 2009. Taste bud development and patterning
862 in sighted and blind morphs of *Astyanax mexicanus*. *Developmental Dynamics* **238**:3056-3064.
863 doi: 10.1002/dvdy.22144
864
865 **Warga RM, Kane DA, Ho RK.** 2009. Fate mapping embryonic blood in zebrafish: multi- and
866 unipotential lineages are segregated at gastrulation. *Developmental Cell* **16**:744-755. doi:
867 10.1016/j.devcel.2009.04.007
868
869 **Wheaton WW, Chandel NS.** 2011. Hypoxia. 2. Hypoxia regulates cellular metabolism.
870 *American Journal of Physiology-Cell Physiology* **300**:C385-C393.
871 doi:10.1152/ajpcell.00485.2010
872
873 **Wei W, Wen L, Huang P, Zhang Z, Chen,Y, Xiao A, Huang, H, Zhu Z, Zhang B, Lin S.**
874 2008. GFi1.1 regulates hematopoietic lineage differentiation during zebrafish embryogenesis.
875 *Cell Research* **18**:677-685. doi: 10.1038/cr.2008.60
876
877 **Weinstein BM, Schier AF, Abdelilah S, Malicki J, Solnica-Krezel L, Stemple, D, Stainier,**
878 **DY, Zwartkruis F, Driever W, Fishman MC**. 1996. Hematopoietic mutations in the zebrafish.
879 *Development* **123:**303-309.

880 **Wells RMG**. 2009. Blood-gas transport and hemoglobin function: adaptations for functional and
881 environmental hypoxia. In *Fish Physiology, Vol. 27* (ed. J.G. Richards, A.P. Farrell and C.J.
882 Brauner). pp. 255–299. New York: Elsevier.
883
884 **Wong-Riley, M**. 2010. Energy metabolism of the visual system. *Eye Brain* 2: 99-116.

885 **Xiong S, Krishnan J, Peuβ R, Rohner N.** 2018. Early adipogenesis contributes to excess fat
886 accumulation in cave populations of *Astyanax mexicanus*. *Dev. Biol*. **441**, 297-304. doi:
887 10.1016/j.ydbio.2018.06.003
888
889 **Yamamoto Y, Stock DW, Jeffery WR.** 2004. Hedgehog signalling controls eye degeneration in
890 blind cavefish. *Nature* **431**: 844-847. doi:10.1038/nature02864.
891
892 **Yoshizawa M, Jeffery WR, van Netten S, McHenry MJ.** 2014. The sensitivity of lateral line
893 receptors and their role in the behavior of Mexican blind cavefish (*Astyanax mexicanus). Journal*
894 *of Experimental Biology* **217**, 886-895. doi: 10.1242/jeb.094599
895
896 **Figures and Legends**

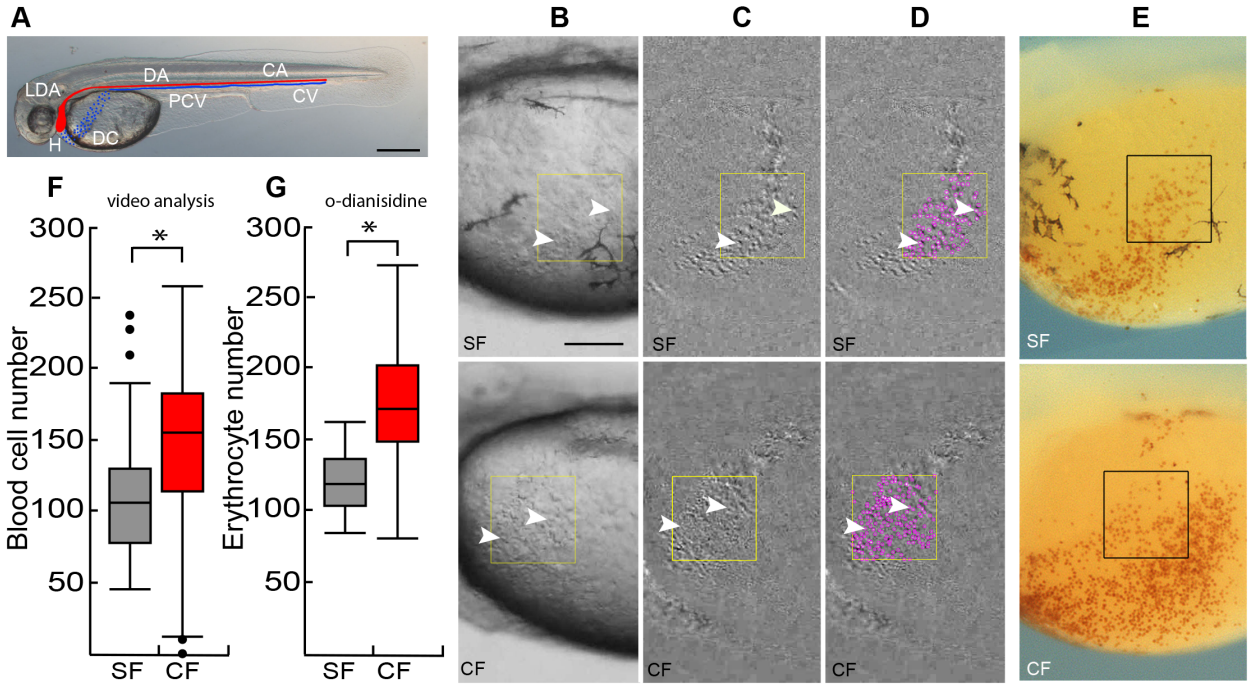

Figure 1. Cavefish have more erythrocytes than surface fish. (A) At 36 hpf blood circulates from the heart (H) through the lateral dorsal aorta (LDA), the dorsal aorta (DA) and caudal artery (CA) (blood flow shown in red), and back to the heart through the caudal vein (CV), the posterior cardinal vein (PCV), and the Duct of Cuvier (DC) (blood flow shown in blue). Scale bar is 200 µm. (B-D). Video analysis of circulating blood cells (arrowheads) in a region of interest (ROI, boxes) in the DC of surface fish (SF) and cavefish (CF) larvae at 36 hpf visualized by subtraction of two video frames 0.15 seconds apart (C, D) and quantified using the plugin TrackMate (ImageJ) (D, purple dots). E. o-dianisidine staining of red blood cells in the DC of surface fish (SF) and cavefish (CF) larvae at 36 hpf. Boxes: erythrocyte quantification regions. Scale bar in E is 100µm, B-E are the same magnifications. (F, G). Quantification of blood cells in the DC by video analysis (F) and o-dianisidine staining. Box plots show the median, quartiles, min-max values and outliers (dots). Asterisks: $p < 0.05$, N = 72 (in F) and $p < 0.0001$, N = 36 (in G). Statistics by Wilcoxon/Kruskal-Wallis Rank Sums test.

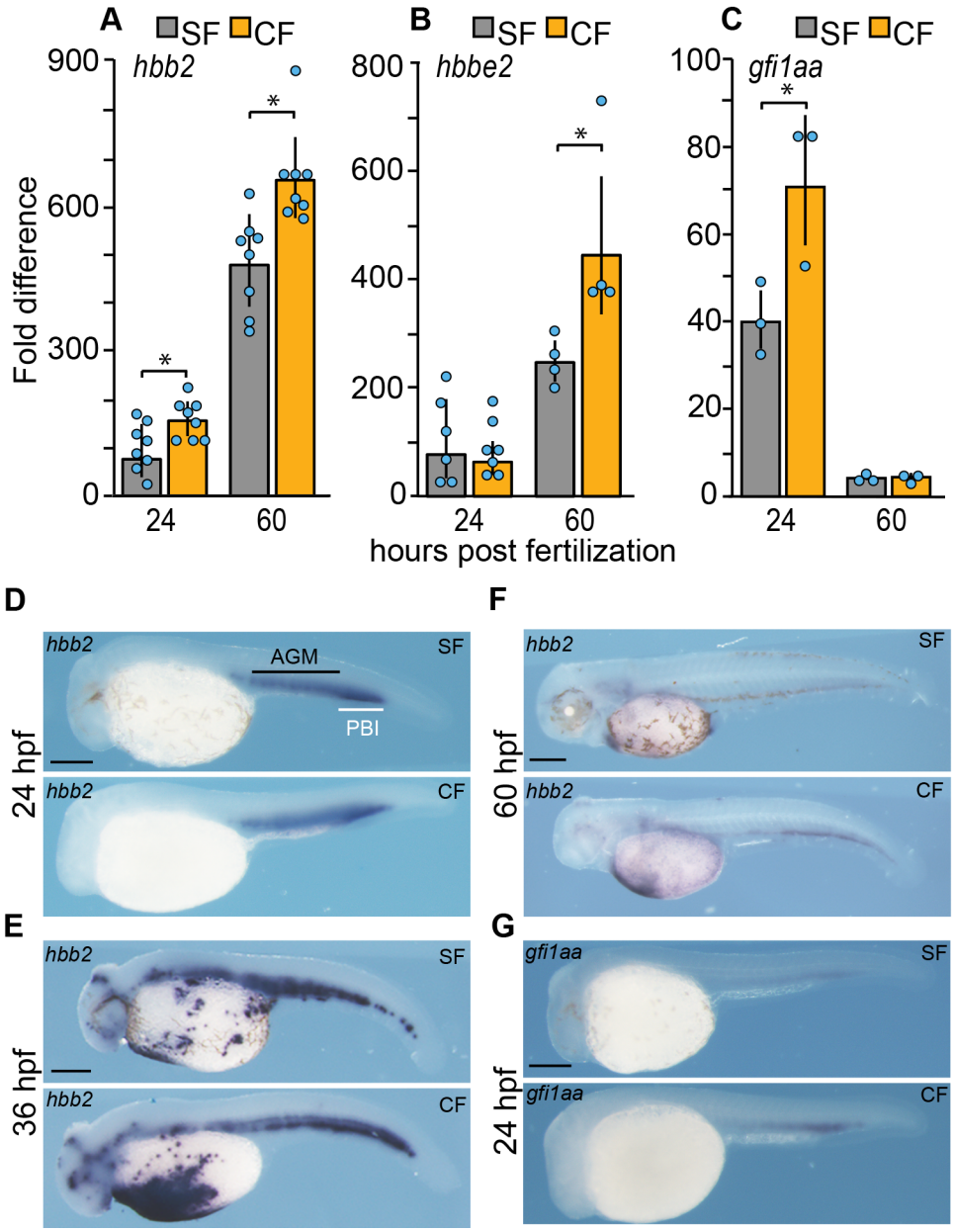

Figure 2. Expression of hematopoietic genes during surface fish and cavefish development. (A-C). qPCR quantification of *hhb2*, *hbbe2,* and *gfi1aa* transcripts in surface fish (SF) and cavefish (CF) larvae at 24 hpf and 60 hpf. Error bars: range of fold change. Asterisks: (A) N = 8. p = 0.0045 for SF vs CF at 24 hpf and p = 0.0254 for SF vs CF at 60 hpf; (B) N = 4. P = 0.0271 for SF vs CF at 60 hpf.; (C) N = 3. P = 0.0413 for SF vs CF at 24 hpf. Statistics by two-way ANOVA followed by Student's t test. (D-G). *In situ* hybridizations showing *hbb2*

919 staining at 24, 36, and 60 hpf, and (D-F) and *gfi1aa* staining (G) at 24 hpf in CF and SF. AGM:

920 aorta-gonad-mesonephros. PBI: posterior blood island. Scale bars are 200 µm in each frame.

921 Magnifications are the same in SF and CF.

922

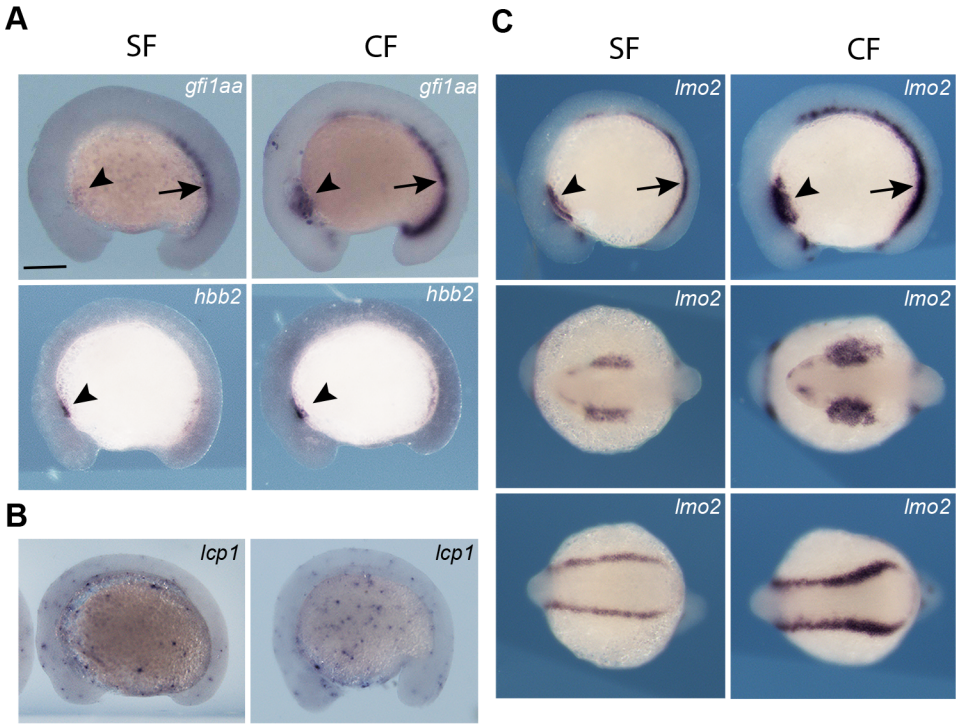

923

924 Figure 3. Hematopoietic domains in 14 hpf surface fish and cavefish embryos. (A). *In*

925 *situ* hybridizations showing expression of the *gfi1aa* (top frames) and *hbb2* (bottom frames)

926 genes in the anterior lateral mesoderm (ALM, arrowheads) and posterior lateral mesoderm

927 (PLM, arrows) in surface fish (SF) and cavefish (CF). (B) Expression of the macrophage marker

928 gene *lcp1* in SF and CF embryos. (C). Expression of the hematopoietic marker gene *lmo2* in the

929 ALM and PLM of CF and SF embryos, and expansion of expression in CF embryos. Scale bar

930 in A is 200µm; magnification is the same in all frames.

931

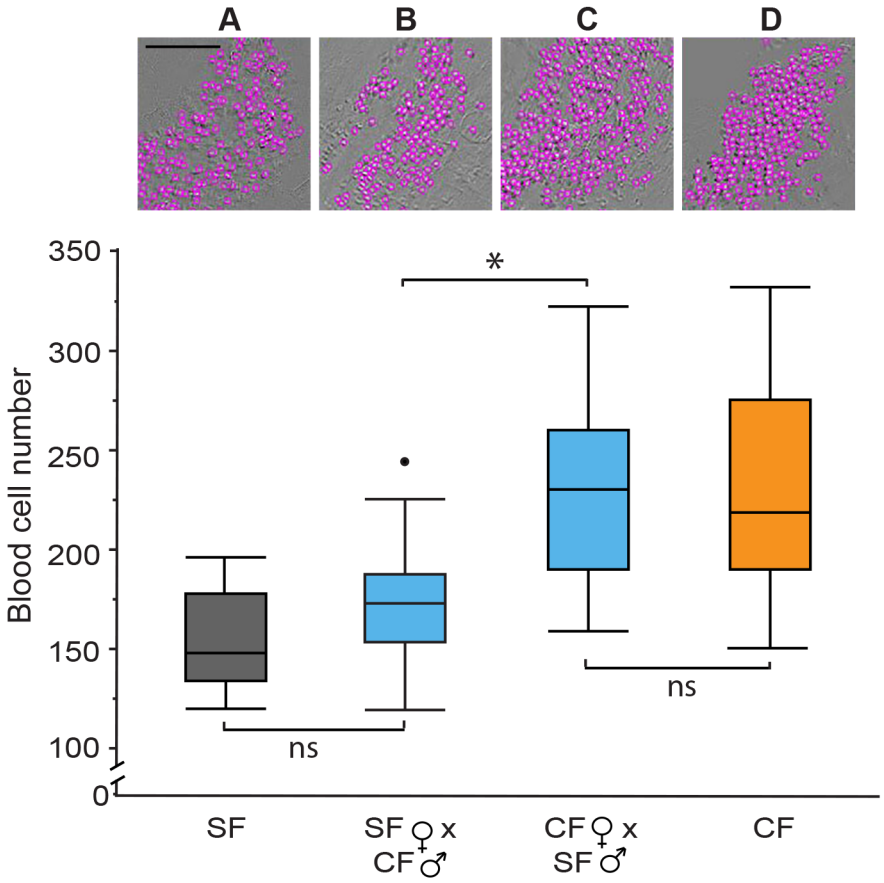

932

933 Figure 4. Maternal control of increased blood cells in cavefish determined by reciprocal

934 hybridizations. Video imaging in the Duct of Cuvier and blood cell quantification at 34 hpf in

935 the F1 progeny of a (A) surface fish (SF) X SF control cross, (B) a SF female X cavefish (CF)

936 male cross, (C) a CF) female X SF male cross, and (D) a CF X CF control cross. (A-D) Top

937 row. Representative images of blood cell number aligned with box plots below. Scale Bar is

938 100µm; magnifications are the same in each frame. Bottom row. Boxplots of blood cell numbers

939 showing medians, quartiles, min-max values, and outliers (dots). Asterisks: $p<0.05$. ns: not

940 significant. N=20 for each box plot. Statistics by Wilcoxon/Kruskal-Wallis Rank Sums test

941 followed by Wilcoxon for each pair.

942

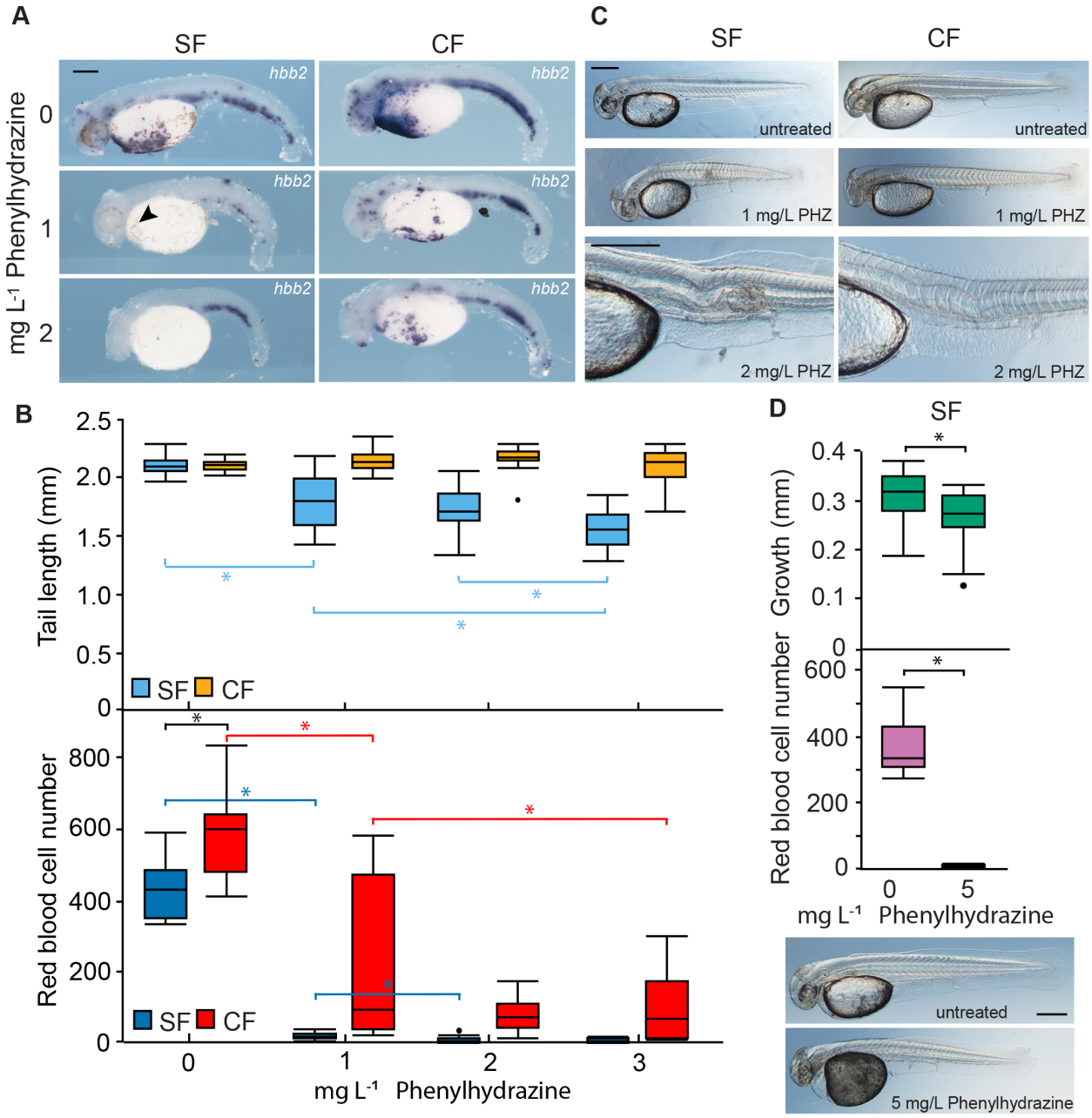

Figure 5. Differential effects of hemolytic anemia on surface fish and cavefish development. (A). *In situ* hybridization with the *hbb2* gene marker in 40 hpf larvae treated with different phenylhydrazine (PHZ) concentrations. Scale bar is 200 µm. Magnification is the same in all frames. (B). Larval tail length (top) and erythrocyte number in the Duct of Cuvier (DC) (bottom) in SF and CF embryos as a function of PHZ concentration. Asterisks in B (top) $p < 0.0001$. N = 23 for SF 0, 2 mg L^{-1} and CF 3 mg L^{-1}. N = 24 for SF 1 and 3 mg L^{-1} and CF 0, 1, and 2 mg L^{-1}.

Asterisks in B (bottom) consecutively from left to right: $p = 0.0197$, $p < 0.0001$, $p = 0.0002$, $p < 0.0001$, and p 0.0102. N = 20 for SF 0, 1, 2 and CF 3 mg L^{-1}. N = 10 for SF 3 mg L^{-1}. N = 19 for CF 0 mg L^{-1}. N = 21 for CF 1 mg L^{-1}. N = 22 CF 2 mg L^{-1}. Statistics by Wilcoxon/Kruskal-Wallis Rank Sums test followed by Wilcoxon for each pair. (C). Axial defects induced by hemolytic anemia in SF and CF embryo. Scale bars are 200 µm; magnifications are the same in top four frames and bottom two frames. Data from B and C were obtained from the same embryos. (D). Effects of a 1 hr. treatment with 5 mg/L PZH on post-anal tail growth (top), erythrocyte number measured in the DC (middle), and axial development (bottom). Scale bar is µm; magnification is the same in both frames. Asterisk (top): $p = 0.0115$, N = 20. Statistics by Student's t test. Asterisk (middle): $p = 0.0001$, N = 10. Statistics by Wilcoxon/Kruskal-Wallis Rank Sums test followed by Wilcoxon for each pair. Box plots in C and D show whiskers (=5%), mean (line) and outlier (dot). SF: surface fish. CF: cavefish. Box plots show the median, quartiles, min-max values and outliers (dots).

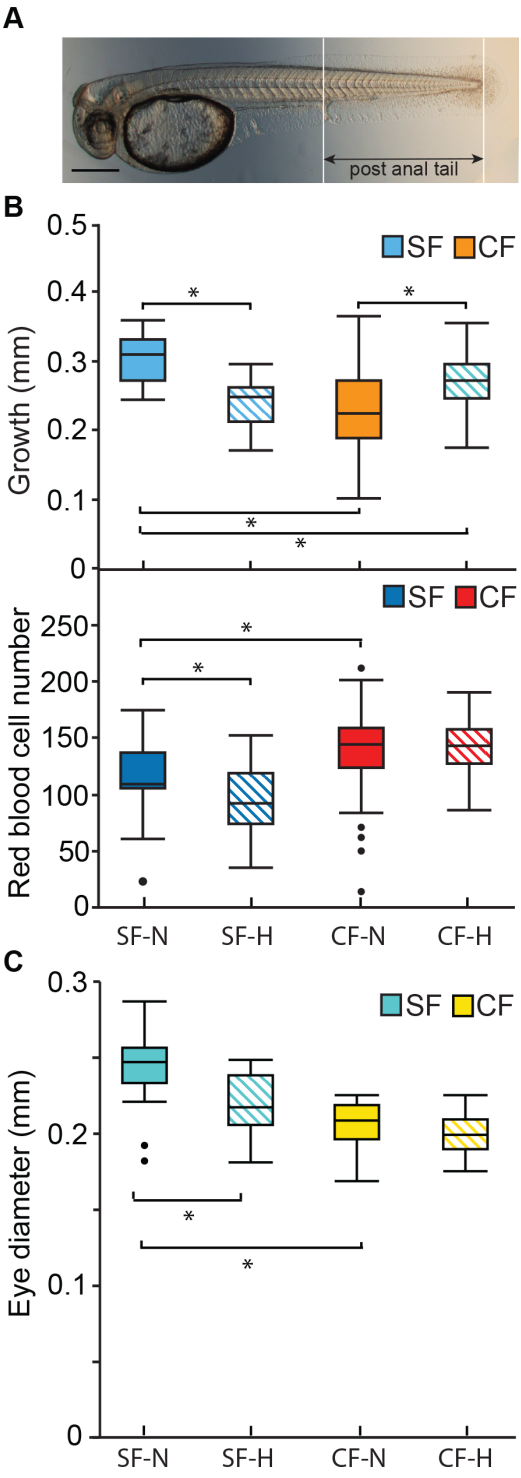

964

965 Figure 6. Effects of laboratory induced hypoxia on surface fish and cavefish growth. (A).

966 Image of a 36 hpf surface fish larval showing post-anal tail length. Scale Bar is 200 µM. (B).

967 Relative post-anal tail growth (top) and erythrocyte numbers (bottom) of surface fish and

968 cavefish over an 18 hr. period under normoxic and hypoxic conditions. Top frame asterisks from
969 left to right: $p < 0.0001$, $p = 0.002$; $p < 0.0001$, and $p = 0.0021$. N = 23 for SF-N and SF-H. N =
970 46 for CF-N. N = 47 for CF-H. Statistics by Wilcoxon/Kruskal-Wallis Rank Sums test followed
971 by Wilcoxon for each pair. Middle frame asterisks from left to right: $p = 0.0116$, and $p = 0.0078$.
972 N = 22 for SF-N. N = 21 for SF-H. N = 47 for CF-N, and N = 45 for CF-H. Statistics by one-
973 way ANOVA followed by Student's t-test. (C) Difference in eye diameters in surface fish and
974 cavefish after 18 hr. of hypoxia or normoxia. Bottom frame asterisks: $p = 0.0002$ and $p < 0.0001$.
975 N = 18 for SF-N. N = 14 for SF-H. N = 30 for CF-N. N = 28 for CF-H. Statistics by one-way
976 ANOVA followed by Student's t-test. Box plots show median, quartiles and min-max values.

977 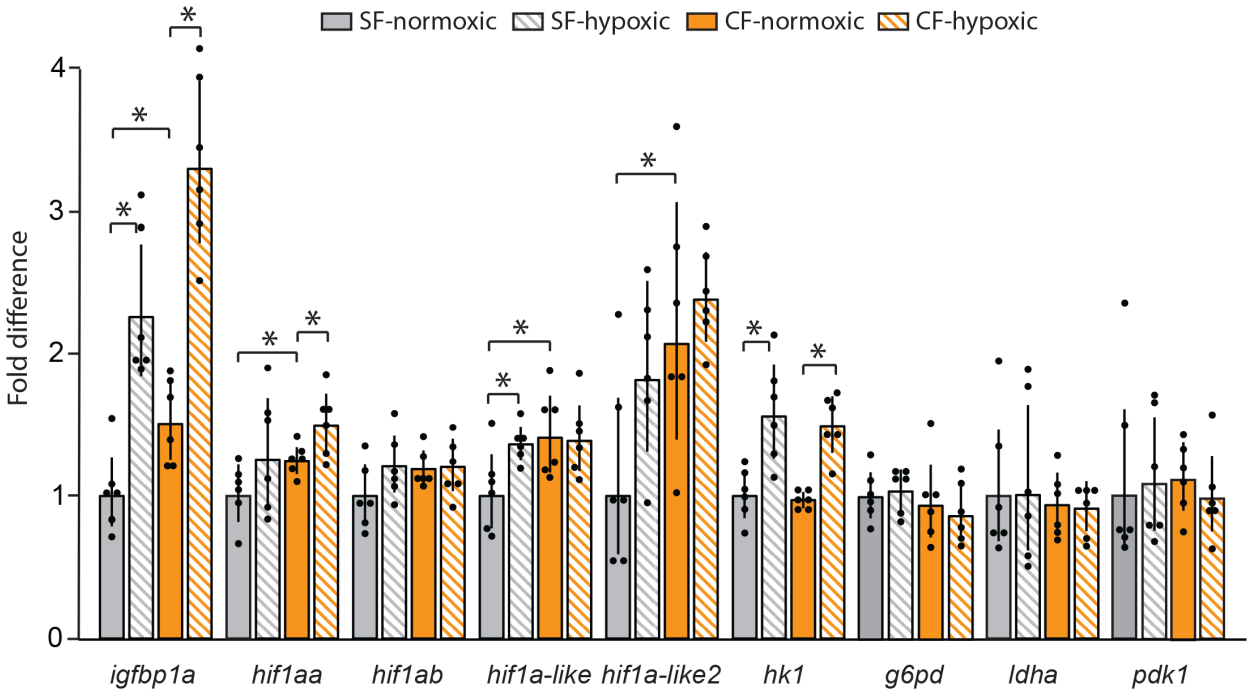

978 Figure 7. Changes in expression of some of the key HIF pathway genes in surface fish
979 and cavefish exposed to hypoxia or normoxia. Bars indicate qPCR fold difference over surface
980 fish in normoxic condition. Error bars: range of fold change. Asterisks from left to right: $p <$
981 0.0001, $p < 0.0001$, $p = 0.0044$, $p = 0.0306$, $p = 0.453$, $p = 0.0155$, $p = 0.0083$, $p = 0.0306$, $p =$
982 0.0002, and $p = 0.0003$. N = 6 for each determination. Statistics by one-way ANOVA followed

983 by Student's t-test (*igfbp1a*, *hif1ab, hif1a-like*, *hif1a-like2*, *hk1*, *g6pd*, *ldha*, *pdk1*) or with

984 unequal variance by Wilcoxon/Kruskal-Wallis Rank Sums test followed by Wilcoxon for each

985 pair (*hif1aa*).

986

987 **Tables**

988 Table 1. Penetrance of abnormalities in phenylhydrazine-treated surface fish and cavefish
989 embryos.
990
991

Morph	PHZ concentration	% edema	% defective notochord
SF	0	0	0
CF	0	0	0
SF	1	4.1	87.5
CF	1	0	41.7
SF	2	75.0	100
CF	2	8.3	87.5
SF	3	95.8	100
CF	3	25.0	100

992 Morph PHZ concentration % edema % defective notochord
993

1002 PHZ: phenylhydrazine. SF: surface fish. CF: cavefish. N = 24 for each morph treatment.
1003
1004
1005 Table 2: Primer sequences used for gene expression analysis with qPCR

1006

rpl13a	GeneID: 103025160	ENSAMXG00000033532	caagtactgctgggccacaaag	aggaaagccaggtacttcaatttgtt
gfi1aa	GeneID: 103029320	ENSAMXG00000006669	agtgtgtgtgatcgaccttcaga	ggacattcttcattgtctggtgacg
hbbe2		ENSAMXG00005017210*	taaatccctctgcagggctctgat	cctgatcacctccggattagccataata

hbb2	GeneID: 111196758	ENSAMXG00000031275	gctcacggtgtagttgttctc	ggatccacgtgcagtttctc
gnb1b	GeneID: 103023031	ENSAMXG00000040710	ctctgctaaactgtgggatgtg	ccgttagggaagaaacagatgg
hif1aa	GeneID: 103022448	ENSAMXG00000039550	cagcaccaacacacacactcaa	gtcactgaccaccagtcctaca
hif1ab	GeneID: 103033873	ENSAMXG00000019342	gcatgggccttacacagttt	gcaccagcatttccctcatt
hif1alike	GeneID: 103027586	ENSAMXG00000008564	tgcctcacctgcttctaactct	agctgtattctcctctggcttga
hif1alike2	GeneID: 103041845	ENSAMXG00000007272	cattctaagttccagcccatcc	cattggctgcaccatctctc
hk1	GeneID: 103028521	ENSAMXG00000012670	ctcaatcggctgaaggacaacaa	agccgtcgagaatactgtggat
g6pd	GeneID: 103035433	ENSAMXG00000017509	tcctactctgtggtggttgtt	gagacggtctgcttcagtatct
ldha	GeneID: 103047177	ENSAMXG00000032467	tgtggtgtccaacccagttgata	agcgagctgagtccaagttagt
pdk1	GeneID: 103033744	ENSAMXG00000039808	tcctcaaccagcacactcttct	agtgacacgacagtgaggatcaa

igfbp1a	GeneID: 103033920	ENSAMXG00000009512	cccaacagaagctggaagataag	ctgcccatccagagttgattc

*blasts to the cavefish genome but also cloned from surface fish in this study

Videos

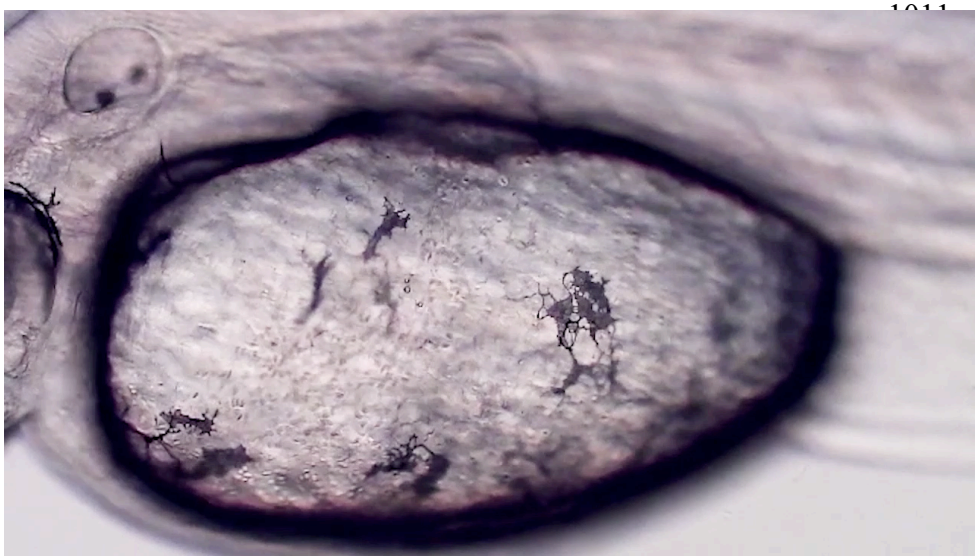

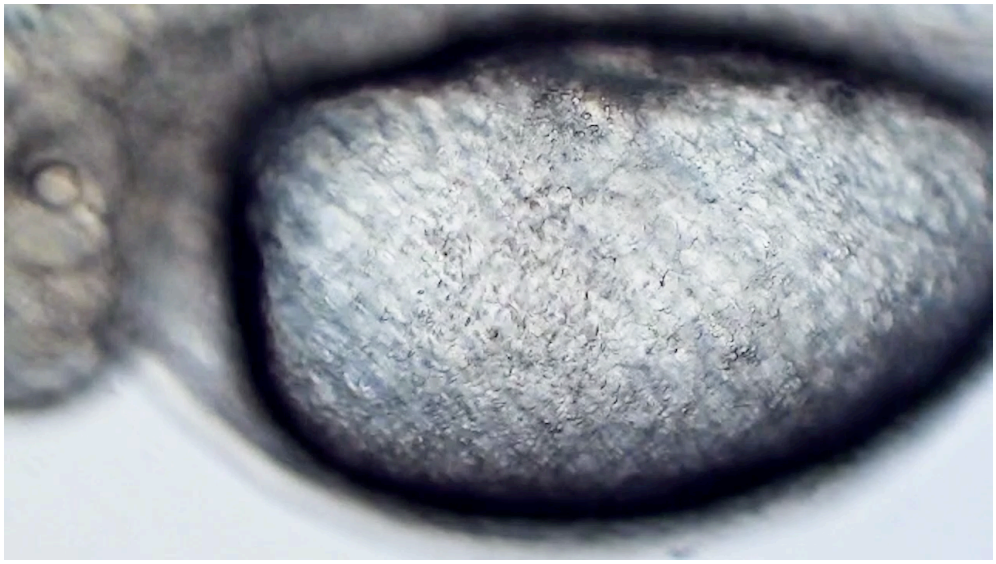

1028 Videos 1 and 2. Blood cells flowing from the cardinal vein through the Duct of Cuvier to the

1029 heart in (1) surface fish and (2) cavefish